TRANSITION PHENOMENA IN OSCILLATING LIQUID COLUMNS

By

JULIAN ROBERT STUART PARK, B.Eng.

A Study Report

Submitted to the Faculty of Graduate Studies

in Partial Fulfilment of the Requirements

for the Degree

Master of Engineering

McMaster University

(May) 1970

MASTER OF ENGINEERING (1969)
(Chemical Engineering)

MCMASTER UNIVERSITY
Hamilton, Ontario.

TITLE: Transition Phenomena in Oscillating Liquid Columns

AUTHOR: Julian Robert Stuart Park, B.Eng. (University of Melbourne)

SUPERVISOR: Dr. M.H.I. Baird

NUMBER OF PAGES: vi, 70

SCOPE AND CONTENTS:

The damping of free oscillations in liquid-filled U-tube manometers was investigated. The laminar damping coefficients determined were in good agreement with those obtained in previous studies; allowances were made for the secondary flow patterns existing. Two Reynolds numbers were used to characterize the onset of turbulence for both fully-developed and boundary layer type velocity profiles occurring in the system. There is evidence that transition in oscillating liquid columns is influenced by the internal tube surface, and the transition height may well be dependent on the damping exponent for the turbulent flow prior to transition.

ACKNOWLEDGEMENTS

The author wishes to acknowledge the assistance of those who contributed to the completion of this project. He is particularly grateful to his research director, Professor M.H.I. Baird whose many helpful suggestions and interest in our discussions were most valuable.

My sincere thanks are also due to the authorities of McMaster University for their financial assistance.

TABLE OF CONTENTS

	Page
SCOPE AND CONTENTS	ii
ACKNOWLEDGEMENTS	iii
LIST OF FIGURES	vi
1. INTRODUCTION	1
2. LITERATURE REVIEW	2
3. EXPERIMENTAL	8
3.1 Experimental Equipment	8
3.2 Experimental Procedure	11
3.2.1 Start-up	11
3.2.2 Experimental measurements	12
4. DISCUSSION OF EXPERIMENTAL RESULTS	14
4.1 Laminar Damping Coefficient	14
4.1.1 Introduction	14
4.1.2 Theory	14
4.1.3 Discussion	17
4.1.3.1 Flow reversal	20
4.1.3.2 Surface tension	21
4.1.3.3 Viscous dissipation in the curved section	22
4.1.3.4 Falling film	23
4.2 Laminar-Turbulent Transition	28
4.2.1 Turbulence mechanism	28
4.2.2 Method of analysis of transition	29

Page

4.2.3 Theory 32

4.2.3.1 Boundary layer regime 32

4.2.4 Discussion 37

4.2.4.1 Method of analysis 37

4.2.4 2 Transition Reynolds number 43

4.2.4.3 Classification of data 48

4.2.4.4 Turbulent damping exponent 51

4.2.4.5 Wavy flow 54

5. CONCLUSIONS AND RECOMMENDATIONS 57

NOMENCLATURE 59

BIBLIOGRAPHY 62

APPENDICES

APPENDIX I 64

A.1 VISCOSITY MEASUREMENT 64

APPENDIX II 66

LIST OF FIGURES

		Page
FIGURE 1:	Manometer with Characteristic Dimensions	10
FIGURE 2:	Damping Factor as a Function of Oscillation Reynolds Number	18
FIGURE 3:	Decrease in Amplitude with Time	24
FIGURE 4:	Transition Height Determination	40
FIGURE 5:	Transition Height Determination	41
FIGURE 6:	Transition Height Determination	42
FIGURE 7:	Transition Reynolds Number vs. Oscillation Reynolds Number	45
FIGURE 8:	Transition Reynolds Number vs. Oscillation Reynolds Number for Classified Data	49
FIGURE 9:	Turbulent Damping Exponent vs. Tube Diameter	52
FIGURE 10:	Turbulent Damping Exponent vs. Oscillation Period	53
FIGURE 11:	Transition Height vs. Frequency (Tube No.4)	55

1. INTRODUCTION

The understanding of the characteristics of pulsating flow is of considerable technological interest since unsteady flow in tubes plays a major role in unsteady state processing, hydraulic and pneumatic control systems, blood circulation and elsewhere.

The liquid-filled U-tube manometer is a simple system, with no net flow component, for studying the phenomena involved and has been used as such by previous investigators.

The present work gives additional information on two aspects of oscillations in U-tubes:

(1) The effect of secondary flow patterns on laminar damping, in particular conditions at the glass/liquid interface (surface tension).

(2) A criterion for the transition from laminar to turbulent flow, indicating a relationship between the turbulent damping exponent and transition.

2. LITERATURE REVIEW

One of the first extensive experimental studies of liquid oscillations in U-tubes was carried out by Menneret (1) in 1911. These experimental results have formed the basis for testing the theoretical equation for manometer response derived by subsequent workers. Since then, it has been recognized that for laminar flow in the system, the fluid motion is characterized by the oscillation Reynolds number:

$$Re_o = \frac{R^2\omega}{\nu} \qquad (2.1)$$

Valensi et al. (2, 3) extensively discussed the relationship between the apparent friction factor (determined by the logarithmic decrement of free oscillations) and this Reynolds number. They identified a number of distinct flow regimes, correlating the measurements of Menneret for low Re_o, where the velocity profile in the tube is fully developed (i.e., parabolic). They showed that as the Reynolds number (Re_o) is increased, a value is reached at which the maximum velocity ceases to occur on the tube axis (Richardson and Tyler's Annular Effect (4)). The flow at high oscillation Reynolds numbers was analysed by Von Karman and Valensi (5) who made use of boundary layer theory, the theoretical equation being in good agreement with experimental results.

Ury (6) obtained an analytical relationship between manometer response parameters and oscillation Reynolds number for a large range of the latter. He obtained experimental results in agreement with the theory which yielded higher damping coefficients (of the order of 20%) than the asymptotic solution of Valensi and Von Karman.

Biery (7, 8) was the first worker to attempt to theoretically account for secondary flow patterns in the U-tube. He modified the equation of motion to include a driving force due to the end effects of surface tension and additional viscous damping caused by flow reversal at the column ends and non-axial flow in the curved section. The equation of motion was then integrated numerically to obtain laminar damping coefficients. Although these end effects corrections had a theoretical basis, they could not be evaluated from theoretical principles alone. That is, the corrections are no more than a fitting factor between the simulated and experimentally determined damping factor.

Another factor which Biery noticed was that the damping was generally higher for the first half-cycle, due to friction occurring when air was expelled from the manometer leg, held under pressure initially. As Menneret's data was determined from this cycle only, it was reasonable to expect his experimental damping factors to exceed the theoretically determined ones.

Richardson (9) investigated the effect of manometer inclination on the laminar damping response of the system. He concluded that the inclination of the tube was not significantly different from the effect of increasing the length of the oscillating liquid column, as both factors increased the period of the oscillations without having any significant effect on the damping. Hence, the increase in free surface area due to tube inclination, does not influence the damping markedly.

Richardson (10) interpreted the oscillation Reynolds number as proportional to the square of the ratio of the tube radius to the oscillating boundary layer thickness, $(\nu/\omega)^{\frac{1}{2}}$. Thus, for large values of this parameter, the viscous effects are concentrated near the walls and the bulk of the fluid moves as if it were frictionless (plug flow). For small Reynolds numbers the boundary layer has become so large relative to the tube radius that velocity gradients are appreciable at all points across the tube. He concluded that for laminar flow the amplitude decay factor can be determined as a function of the oscillation Reynolds number provided the effects of surface tension and tube curvature can be neglected.

The transition from laminar to turbulence in steady-state pipe flow has been studied by numerous workers. The original concepts of the onset of turbulence provided by Hagen, Reynolds, Schiller, Tollmien and Schlichting are very well summarized in a paper by Lindgren (11), which includes

detailed references to the original publications. The observation of turbulent flashes by Reynolds, and Tollmien's "Theory of the Instability of Small Oscillations" will be discussed later as a basis for an understanding of the onset of turbulence in oscillatory flow. In steady pipe flow, the criterion for transition is the value of the pipe Reynolds number given by:

$$Re_p = \frac{Du_m}{\nu} \tag{2.2}$$

In normal engineering practice, $Re_p \approx 2000$ at transition, but with specially smoothed flows, laminar conditions can persist at much higher values.

The transition from laminar to turbulent flow in unsteady U-tube operation, unlike the transition from fully developed to boundary layer laminar flow in the system, has been studied to a far smaller extent. Richardson (9) characterized the transition with the use of a kinematic Reynolds number:

$$Re_h = \frac{h^2\omega}{\nu} \tag{2.3}$$

When this number is very small the flow is laminar and turbulence is set up as the parameter increases. The value of the transition amplitude (h_T) can be easily determined by using an analysis (12) where the turbulent damping is assumed to be proportional to a constant power of velocity, greater

than unity, for all oscillation heights. Richardson found that transition occurred at a kinematic Reynolds number of the order of 100,000. However, the transition value of Re_h was very sensitive to small geometric changes within the tube. When one of the glass tubes was fractured at the bottom of the U and rejoined with rubber tubing (with a small gap between the parts), the transition value was decreased by 50%.

Richardson also investigated the effect of variation of tube cross-section by constructing a U-tube with unequal diameter vertical legs. The damping was found to be independent of the flow direction in each half-cycle and to be turbulent even at the lowest Reynolds number tested (Re_h = 9000).

Richardson was unable to reach any general conclusions about the influence of the kinematic Reynolds number on laminar stability. However, he agreed with Christopherson et al. (22) in doubting that the criteria for laminar-turbulent transition in steady pipe flow could be directly applied to the oscillating U-tube system. Also, he was unable to find any internal evidence for the assumption that the damping force is proportional to the n^{th} power of the velocity in the turbulent regime, for all oscillation heights. This is an inherent assumption in his method of determining the transition height.

Ury (6) also investigated the onset of turbulence in the manometer system and in his case correlated the results in terms of a modified "kinetic" Reynolds number for oscillatory flow:

$$R_k = \delta' Re_p \qquad (2.4)$$

where the value of δ' depends on the type of flow:

$\delta' = \sqrt{2}$ for laminar flow,

$\delta' \approx 1$ for turbulent flow.

Experiments indicated that transition to turbulence occurred when the modified kinetic Reynolds number R_k exceeded a critical value which was a function of the oscillation Reynolds number ($R^2\omega/\nu$). This criterion can be used to determine the maximum amplitude h_T which the oscillating liquid column will tolerate without transition to turbulence.

Ury was able to summarize his results in a diagram of friction factors (log f vs log R_k) for pulsating flow, which is analogous to the well-known plot of log f vs log Re_p for steady pipe flow.

Binnie (13) investigated the effect of oscillation on transition for pipe flow; his results were inconclusive.

Baird (14) investigated pulsed flow past a cylinder and obtained a functional relationship between the separation Reynolds number ($D\omega A/\nu$) and the oscillatory Reynolds number, the exponent being 0.8.

3. EXPERIMENTAL

3.1 Experimental Equipment

The U-tubes used in the experimental study were formed from soft glass tubing and had the dimensions shown in Fig 1 and Table 1. Before use, the tubes were thoroughly cleaned with chromic acid to yield a reproducable surface, and hence, give rise to a uniform liquid film during operation. All but one of the manometers had a geometrically similar basis, the ratio of radius of curvature of the curved section to tube radius being 10 : 1. The one exception was tube 2, which had a ratio of 2 : 1 and was used solely to determine the importance of this parameter. The radius of the bend was made as large as reasonably possible to minimize the distortion of streamlines in the curved section. With a small radius of curvature a significant secondary flow perpendicular to the longitudinal axis would exist. In making the bends, the tubing was slightly necked down in the curved region. An average tube radius was determined by weighing the quantity of water necessary to fill the manometer, between the two symmetrical positions of maximum initial release of the liquid column.

The U-tubes were clamped into a vertical position, in front of a scale on which were later marked the amplitudes of the oscillations. The clamping was such that no vibrations

were transferred to the tube during the start-up operation.

Auxiliary items of equipment used were: a mercury thermometer for recording liquid column temperatures to within ± 0.1°C; an electric stop watch for measuring oscillation cycle times to an accuracy of ± 0.01 sec; rubber tubing for supplying air pressure or vacuum to one leg of the manometer in order to achieve a steady initial displacement. The amplitudes of the moving fluid were measured to within ± 0.02 inches.

The viscosity of the liquids was measured with a capillary viscometer (See Appendix I). This apparatus both determined the magnitude of the liquids' kinematic viscosity and checked that the liquid was in fact Newtonian. The data obtained on this viscometer for toluene checked to within ± 2% of the values presented in the standard table (17) and as a result the tabluated values for water, toluene and methanol were used. For the toluene-paraffin mixtures the experimentally determined values were used.

FIGURE 1: MANOMETER WITH CHARACTERISTIC DIMENSIONS

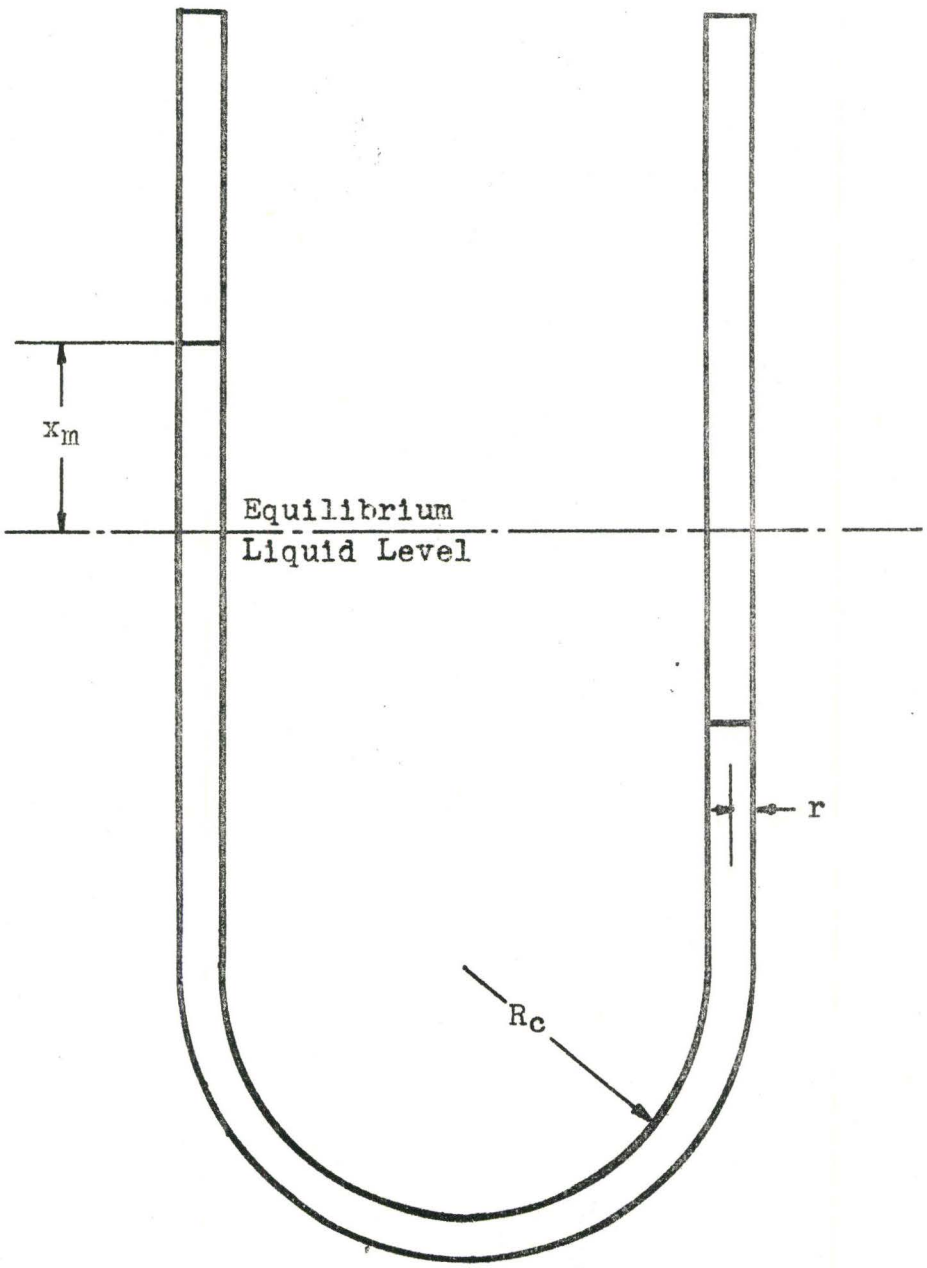

TABLE 1

TUBE DIMENSIONS

MANOMETER NUMBER	NOMINAL I.D.	ACTUAL I.D.	R_c	MAXIMUM LENGTH
	(cm)	(cm)	(cm)	(cm)
1	0.60	0.60	3.00	122
2	0.60	0.60	0.90	122
3	1.00	1.00	5.00	99
4	1.00	1.00	5.05	372
5	1.50	1.49	7.65	114
6	1.90	1.89	10.00	120

3.2 Experimental Procedure

3.2.1 Start-up

The legs of the manometer were brought into imbalance by applying air pressure (or vacuum), through rubber tubing to one of the legs. A rubber stopper was then placed in the other leg, the source of air pressure removed, and the liquid column lowered to the desired starting position by allowing some air to slowly enter the stoppered leg. With the column stationary at the desired starting height, the stopper was quickly removed and the liquid allowed to oscillate freely. Thus, no air flow restriction existed at the end of the tube. However, on the first half-cycle of the

oscillation, some additional damping existed while the higher pressure air flowed out of the U-tube.

In all cases, the oscillations were commenced from the same initial height and amplitude measured after each successive half-cycle. The oscillations were not started from the lower positions as film formation, and its effect on damping, was critically dependent upon the starting position. This was particularly important for water which forms an irregular film. Due to the added damping in the first half-cycle, this point was excluded from the subsequent analysis.

3.2.2 Experimental measurements

The oscillation periods were determined by measuring to the nearest 0.01 sec the time required for the liquid to oscillate from initial start-up to the end of, in general, 10 cycles. For the more viscous solutions and smaller bore tubes, often the period was based on only five cycles, as the damping was more severe in these cases.

The successive peak heights were marked manually on the manometer scale. By repeating every run up to ten times and averaging the values, reproducible results were obtained in spite of the limited accuracy of each individual measurement. The equilibrium height was also recorded immediately the oscillation ceased. Due to the hold-up of liquid in a film on the tube wall, the instantaneous equilibrium position

depended on the initial displacement of the column. The amplitude was then calculated by subtracting the instantaneous equilibrium height from the peak height.

In cases where the damping was severe, the oscillations had to be repeated with different initial heights to yield sufficient data points in the turbulent regime. With this in mind, the data was roughly analysed to ensure that there were sufficient points in each regime before moving to a different system.

4. DISCUSSION OF EXPERIMENTAL RESULTS

4.1 Laminar Damping Coefficient

4.1.1 Introduction

In order to gauge the accuracy of the experimental procedure and measurements, the manometer response in the laminar flow regime was compared with the experimental and theoretical findings of previous workers. With the accuracy of the method confirmed by this check with previous results, the analysis of results for the laminar-turbulent transition could be undertaken with greater confidence.

4.1.2 Theory

Liquid filled U-tube manometers with laminar damping are typical examples of linear physical systems of second order, the approximate differential equation being:

$$\ddot{h} + j\dot{h} + bh = F(t) \qquad (4.1)$$

If the analysis is limited to laminar flow where only small displacements occur in the column, such that disturbing effects arising at the ends and in the curved section are insignificant, equation (4.1) can be transformed into the appropriate standard form:

$$\ddot{h} + 2\zeta\omega_n\dot{h} + \omega_n^2 h = \omega_n^2 h_d \qquad (4.2)$$

The solution of equation (4.2) for free oscillation ($h_d = 0$) is:

$$h = \frac{h_i}{\sqrt{1-\zeta^2}} \left\{ \sin\left[\omega t \sqrt{1-\zeta^2} + \tan^{-1}\left(\sqrt{1-\zeta^2}/\zeta \right) \right] \right\} \exp(-\zeta \omega t)$$

The physical significance of the parameter ζ can be seen if equation (4.2) is considered as a momentum balance. Then the coefficient ($2\zeta\omega_n$) represents the ratio of viscous shear along the column to the column mass. In order to evaluate the parameters, simplifying assumptions as to the velocity distribution in the U-tube system must be made.

A theoretical calculation of manometer response was made by Valensi (2) in 1947. The velocity equation that Valensi used was based on a velocity profile which involved a first kind Bessel function dependence on radial position and incorporated a sinusoidal amplitude variation with time. Coupling this with the equation of motion for the system and assuming Poiseuille law fluid friction, the following damping factor equation was derived:

$$\zeta = 2.892 \left(\frac{R^2 \omega_n}{\nu} \right)^{-1} \qquad (4.3)$$

In 1948, Valensi and Von Karman (5) applied the Boundary Layer Theory to obtain an asymptotic solution for very small damping factors. They assumed that the fluid remained stationary and the tube moved with a sinusoidal motion. They were able to solve the equation of motion, simplified by using boundary layer approximations. The

boundary conditions were a sinusoidal variation of velocity at the wall with time and zero velocity at points outside the boundary layer. The resulting equation was:

$$\zeta = \frac{1}{\sqrt{2}} \left(\frac{R^2 \omega_n}{\nu} \right)^{-\frac{1}{2}} \qquad (4.4)$$

In 1962, Ury (6) used a different approach to the problem of manometer response. He assumed rotational symmetry with respect to tube axis in the straight leg such that all "particles" located on a cylinder of radius r will have a time t, the same velocity u = f(r,t). With this assumed velocity profile, two simultaneous differential equations were solved: the standard second-order damped harmonic differential equation (4.2) and the Navier-Stokes equation, which in this case is of the form

$$\nu \left[\frac{\partial^2 u}{\partial r^2} + \frac{1}{r} \frac{\partial u}{\partial r} \right] - \left[\frac{\partial u}{\partial t} + \frac{2gh}{L} \right] = 0 \qquad (4.5)$$

the appropriate boundary conditions being:

(i) zero velocity at the tube wall,

(ii) meniscus height is independent of radius.

The solution of the coupled differential equations contains Bessel functions of the first kind of order zero and one. For the exact expression for the damping ratio see Appendix I of Ury's paper (6).

In practice, it was found that the Bessel function series converged to within one per cent of the exact solution if only the first 100 terms were used to evaluate the damping coefficient.

In 1963, Biery (7) calculated the damping ratio by numerically integrating the equation of motion for the U-tube system. In his solution he attempted to account for the difference between experimental and simulated results by introducing a term in the equation of motion which allowed for the effect of flow reversal at the ends of the oscillating column of fluid. This technique allows for the initial build-up of velocity profile and leads to larger damping factors than the asymptotic solutions.

4.1.3 Discussion

In order to test the accuracy of the experimental results, the damping ratios of the manometer systems were plotted as a function of the Reynolds number $R^2\omega/\nu$ in Fig. 2. An ambiguity arises in making a comparison with the theoretical calculations, as the experimental damping factor is based on the second order system in the damped state, whereas the asymptotic solutions refer to an undamped state ($\zeta = 0$). However, for linear damping, an inherent assumption in the analysis, the experimental logarithmic decrement is related to the theoretical coefficient thus:

FIGURE 2: DAMPING FACTOR AS A FUNCTION OF OSCILLATION REYNOLDS NUMBER

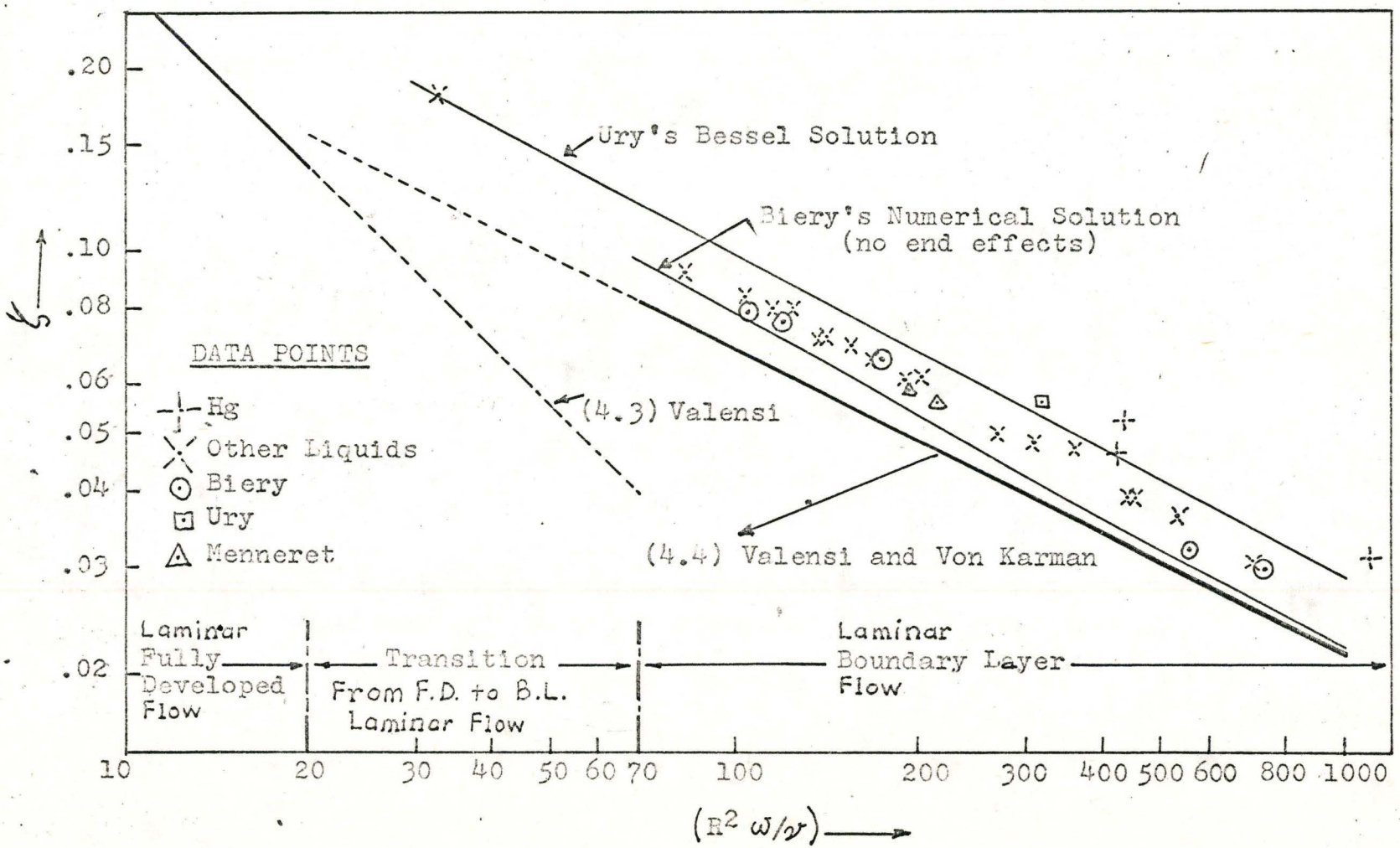

$$\Delta^2 = \zeta^2(1 - \zeta^2) \tag{4.6}$$

where

$$= \frac{1}{\pi} \ln \left| \frac{x_m}{x_{m+1}} \right| \tag{4.7}$$

Moreover, for the small damping coefficients found at high Reynolds numbers the experimental accuracy justifies equating damping factor and the logarithmic decrement.

The lowest Reynolds number (Re_o) investigated was 32 in Run 25. Thus, the accuracy of the asymptotic solution, equation (4.3), for the fully developed flow regime could not be checked. Actually, with the liquids and U-tubes available, experimental laminar damping coefficients for $Re_o \ll 20$ could have been obtained, but it would have been virtually impossible to determine meaningful transition heights due to the severe damping at the large displacements involved.

All the experimental results lie above the theoretical asymptotic solutions. The damping coefficients agree extremely well with the experimental values of Biery (7). This is probably because the systems used in both cases were similar. One point obtained by Ury (6) is interesting, seen in the middle of Fig. 2 at Re = 337. This point was for mercury in a plastic U-tube of diameter 6 mm and gives a significantly higher coefficient than predicted by the theoretical equations. This was also found in the present investigation for mercury/glass systems in Runs 1, 2 and 3.

This suggests added damping due to surface tension effects in small diameter tubes. Menneret's (1) data for the boundary layer regime ($Re_o > 70$) also substantiates these experimental results. In his case, the data was obtained from the first cycle only. This cycle is the poorest one due to start-up effects, although in Menneret's case these effects seem to have been small. However, the fact that he found the damping to be a function of the initial leg differential, indicates the influence of air expulsion in the first stroke.

The reason for the higher experimental damping coefficients indicated on Fig. 2 is additional damping in practice due to flow reversal and assymetric surface tension forces at the column ends, viscous dissipation in the curved bend section, and film formation on the tube walls; the importance of each is now discussed.

4.1.3.1 Flow reversal

According to Biery (7) the reason why the experimentally determined damping coefficients are higher than the theoretically predicted values is mainly due to the secondary flow patterns caused by flow reversal at the ends of the oscillating column. Liquid stationary at the tube walls must suddenly accelerate and flow along the meniscus surface into the high velocity central portion of the stream, and this secondary flow pattern increases the liquid friction.

The reversal end effect was observed experimentally by

watching the flow of particles in the fluid as it flowed up the centre and out towards the wall of the tube, across the meniscus surface. This observation was similar to that found by Valensi and Clarion (15, 16) who made an exhaustive study of the secondary flow patterns at the column ends in oscillating flow.

From equation (4.2) it can be seen that the principal contribution to the damping factor is the viscous force per unit length of the tube times the column length. Thus, an increase in the damping coefficient above the theoretical could be interpreted as an increase in the effective viscous length of the column. A reasonable value for the equivalent length added to the column due to flow reversal would seem to be of the order of a tube diameter. However, analysis of the simulated results shows that the correction necessary would be of the order of 10 tube diameters and tends to suggest that other factors are also important.

4.1.3.2 Surface tension

Another reason for added damping in practice is the retarding surface tension force which occurs when the contact angles between the liquid and the manometer tube are not equal at both ends of the fluid column. With a fluid which wets the walls, the contact angle of both menisci is close to zero and the retarding force is negligible. However, with non-wetting liquids such as mercury, the contact angle at

both ends is considerably different and there is a significant increase in the damping factor as verified by the results for Runs 1, 2 and 3, and the mercury points of Ury.

4.1.3.3 Viscous dissipation in the curved section

Runs 1 and 2 for mercury in a 6 mm diameter tube with different radii of curvature show no significant difference in damping coefficient. It was expected that a larger coefficient would have been obtained with tube number 2 (smaller bend radius) as distortion of streamlines and the associated viscous dissipation would have been much longer. However, it must be remembered that as the oscillation Reynolds number is of the order of 500 for these cases, the velocity profile is markedly "boundary layer" in nature and the curvature would not be as important as for a fully developed profile. Because of the effect of the solution's viscosity on the boundary layer growth, the fact that the U-tubes are geometrically similar may not be a good basis for comparison of systems. However, Runs 1 and 2 together with Biery's calculations do indicate that the effect of viscous dissipation in the curved region for laminar boundary layer flow is small. Further experimental data for large diameter tubes of different radii of curvature, at low values of $R^2\omega/\nu$, would elucidate the importance of viscous dissipation in the curved region, and its effect on laminar damping.

4.1.3.4 Falling film

When the fluid wets the walls of the tube (all liquids except mercury) a film is left by the receding liquid column which is partly picked up by the rising liquid on the return stroke. This effectively reduces the mass of the system and also alters the instantaneous equilibrium position for the U-tube column.

As previously mentioned, in order to obtain correlatable results, the experimental procedure had to incorporate a method of allowing for the effect of film formation on the measured amplitudes. When no correction was made, it was found that, with a negative peak height in the measuring arm, the amplitude was increased, due to film formation, by an amount which made subsequent analysis meaningless (Fig. 3).

However, in order to check that liquid film formation was in fact the reason for the apparent large experimental scatter, an approximate theoretical calculation of apparent increase in column displacement, due to the film, was made.

This calculation was simplified by considering an analagous case of liquid flowing down a plate which is subjected to a sinusoidal withdrawal motion.

In this case, for laminar flow in the film, its thickness is given by (18); for a constant withdrawal velocity:

$$\delta_f = \sqrt{\frac{2\nu u}{g}} \qquad (4.8)$$

FIGURE 3: DECREASE IN AMPLITUDE WITH TIME

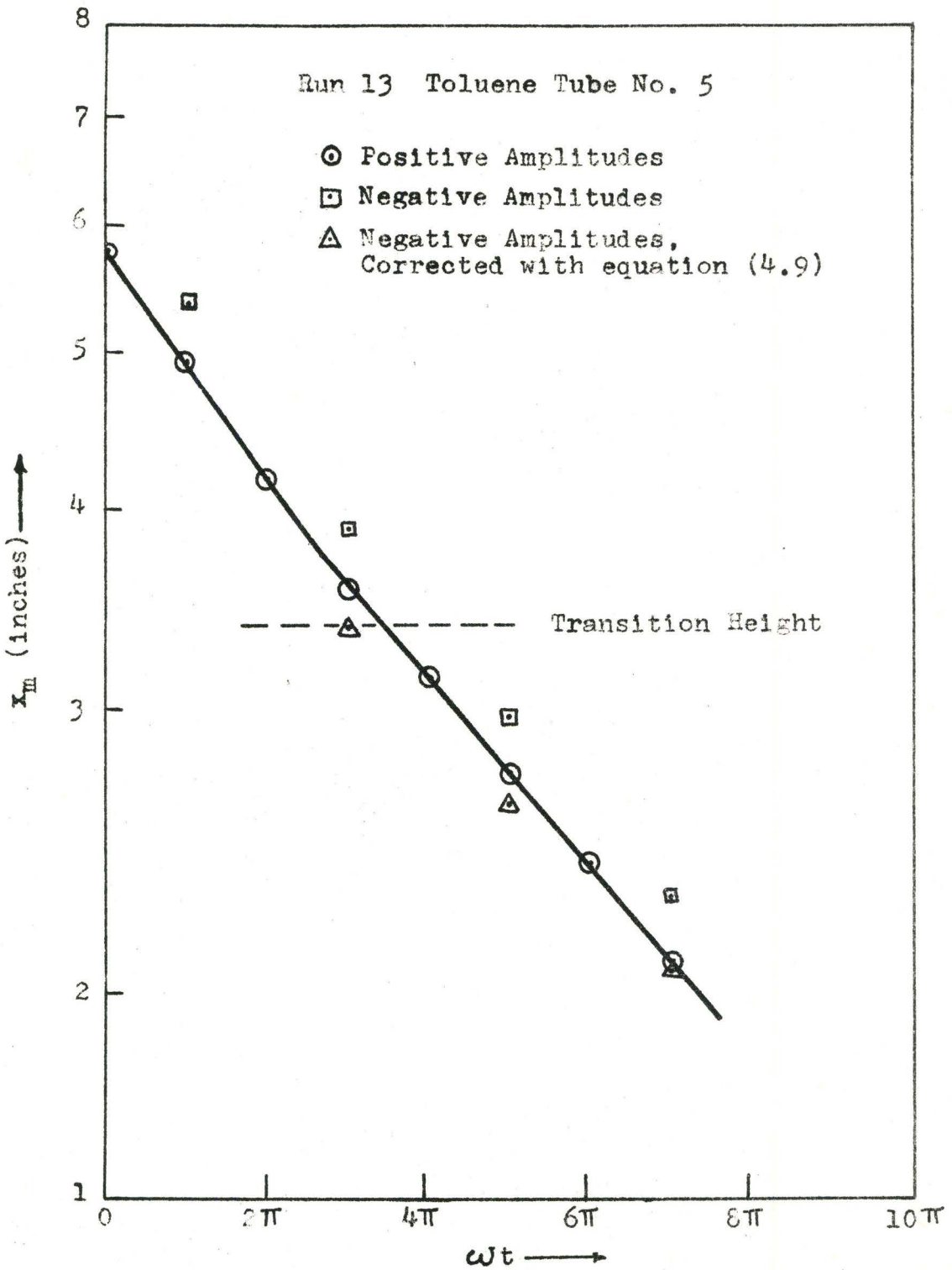

For a sinusoidal motion of the plate, the fluid velocity is:

$$u = A\,\omega \sin \omega t$$

Then the volume of the film adhering to the surface of the plate in time dt is:

$$u\,\delta_f dt \qquad \text{(per unit perimeter)}$$

$$= A\,\omega \sin \omega t \sqrt{\frac{2\nu A\,\omega \sin \omega t}{g}}\; dt$$

The total volume of the film adhering in a half-cycle then is:

$$\int_0^{\frac{\pi}{\omega}} (A\,\omega \sin \omega t)^{3/2} \sqrt{\frac{2\nu}{g}}\; dt$$

$$\approx 1.748\, A^{3/2} \omega^{\frac{1}{2}} \left(\frac{2\nu}{g}\right)^{\frac{1}{2}}$$

assuming that $\delta_f \ll D$ (which checks reasonably for the lower viscosity liquids used); in the U-tube case, the apparent increase in column displacement is given by:

$$h_f = \frac{7.0}{D}\sqrt{\frac{2h^3 \omega \nu}{g}} \qquad (4.9)$$

This correction was applied to the data for Run 13 (Fig. 3). The correction was accurate for small amplitudes but overestimated the film importance at the start of the oscillations. The reason for the error at large oscillation

amplitudes was possibly due to the break-down of the laminar film assumption. The presence of wavy flow (20) in the film was observed even when the flow in the column proper was laminar, as indicated by the transition height analysis. However, equation (4.9) does give an estimate of the effect of film formation on the instantaneous equilibrium height, and indicates that this is the reason why the data is difficult to correlate without correcting for film hold-up.

From Fig. 3, it was found that the easiest way to correlate the results was to use only positive peak heights relative to the equilibrium position, and to record the instantaneous equilibrium position. When the film hold-up was small the instantaneous equilibrium position was constant (to within experimental error) and was recorded only when the oscillations had naturally damped out. For large film hold-ups, the instantaneous equilibrium position was measured after each half-cycle by forcibly stopping the oscillating liquid column. This method gave similar results to that used by Biery (7), where an average of the positive and negative heights was used as a measure of the amplitude for the analysis. The transition heights (See next section) given by the two methods of allowing for film formation, agreed to within 5%, that is, within the experimental error involved. Thus, the method of only measuring positive displacement peaks from equilibrium, and the instantaneous equilibrium position, was used as it involved the collection of considerably fewer data

points and seems to give an equally meaningful turbulent-laminar transition height.

The most difficult film correction to make would have been for water, which formed a very irregular film. With the tube freshly cleaned with acid, the water tended to form droplets at various points on the surface. As the tube walls became contaminated with time a more uniform film was formed. However, the damping coefficients determined from the manometer response of the water/glass system, were in similar agreement with the asymptotic theoretical equations as for those of other solutions (See Fig. 2). This tends to indicate that film formation has an insignificant effect upon damping in laminar flow, as Biery previously concluded.

To conclude, this analysis has shown that the experimental data for the laminar regime of the oscillations is in agreement with that of previous workers and for the boundary layer regime the numerical solution of Biery does appear to be the best theoretical equation. The higher damping coefficients yielded by Ury's Bessel formulation, although good for mercury where surface tension increases the damping, may be due to the initial assumption that the axial velocity is only a function of radial position and time. However, the numerically determined velocity profiles (Biery) indicate that the velocity has a marked dependence on axial position also, which seems reasonable.

4.2 Laminar-Turbulent Transition

4.2.1 Turbulence mechanism

For steady flow in a pipe, the spontaneous onset of turbulence is currently explained by Tollmien's "Theory of the Instability of Small Oscillations" (11) thus: Laminar flow at the tube inlet possesses a planar velocity profile which during passage through the tube tends to parabolic (Poiseuille Distribution). The entrance flow is disturbed by variations of a large range of frequencies (in the case of manometers, due to the irregular motion of the meniscus at high amplitudes). At low Reynolds numbers the velocity profile is stable to most disturbances, whose original intensity determines the time taken for them to fade away as they progress down the tube. However, certain velocity profiles, developed along the entrance length, might become unstable to oscillations of a critical frequency. The disturbances then would increase in amplitude as they proceeded and finally, after travelling the necessary distance of accummulation, lead to the break-down of predominantly steady laminar flow. The collapse of these entrance flow disturbances has been observed experimentally (11) in the form of so-called turbulent flashes, which appear in the shape of asymmetrical toroidal vortices. However, the disturbed entrance region is to be distinguished from the self-maintained turbulent flow which possesses a different structure of small-scale, high energy eddies.

It seems likely that a similar mechanism would apply in the unsteady operation of the manometer. In this case, when the amplitude is large, the liquid film formed on the tube wall, as the column recedes, is wavy in nature. This may well cause disturbances in the fluid proper, which would lead to the break-down of laminar flow.

Also, another probable mechanism is the promotion of turbulence within the boundary layer throughout the tube due to vorticity at the bend and surface roughness.

Thus, there are two distinct turbulence promoters in the system: surface effects at the ends of the liquid column, and irregularities in the boundary layer throughout the tube.

4.2.2 Method of analysis of transition

The motion of the U-tube system undergoing free oscillations with damping proportional to the n^{th} power of velocity ($n > 1$) is described by the following equation:

$$\frac{d^2x}{dt} + j\frac{dx}{dt}\left|\frac{dx}{dt}\right|^{n-1} + b^2x = 0 \qquad (4.10)$$

Richardson (12) has presented a method of analysis from which the turbulent to laminar transition height can be determined, by finding the point at which the damping exponent (n) changes from one to a higher value.

At the completion of each half-cycle (when $\dot{x} = 0$), let $x = x_1, x_2, x_3 \ldots x_m \ldots$ successively, so that after one cycle the amplitude then is x_2

The characteristic solution of equation (4.10) is for a half-cycle, and the logarithmic decrement should be based on a half-cycle, rather than a full cycle as in the case of linear damping (n = 1).

From dimensional analysis the half-cycle amplitude decay may be written:

$$\frac{x_{m+1}}{x_m} = f\left(n, \frac{j x_m^{n-1}}{b^2 - n}\right) \tag{4.11}$$

Richardson (12) has shown that the asymptotic solution of equation (4.10) for the characteristic half-period is:

$$\frac{x_{m+1}}{x_m} = \exp\left(-F(n)\frac{j x_m^{n-1}}{b^2 - n}\right) \tag{4.12}$$

where, for non-integer values of n

$$F(n) = \frac{\pi}{2^{n+1}} \frac{\Gamma(n+2)}{\left\{\Gamma\frac{n+3}{2}\right\}^2} \tag{4.13}$$

While the solution is asymptotic, the deviations due to finite damping are found to be small in practice; for only oscillations with small damping will yield sufficient half-period amplitudes to give an accurate correlation.

In the interpretation of experimental measurements of amplitude decay, the logarithmic decrement should be

calculated from two successive half-cycle amplitudes.

The value of n can be estimated as follows. The logarithmic decrement can be written:

$$\delta_{xm} = \log \frac{x_{m+1}}{x_m}$$

$$= - F(n) \frac{j x_m^{n-1}}{b^{2-n}}$$

Hence $$\delta_{xm} \propto x_m^{n-1}$$

and $$\log (-\delta_{xm}) = (n - 1) \log x_m + \text{const} \qquad (4.14)$$

Thus, a graph of $\log (-\delta_{xm})$ against $\log x_m$ has a slope of $(n - 1)$. The slope of the graph was evaluated by the method of least squares, for both laminar and turbulent regions. In this manner, an error in one particular half-cycle amplitude tended to be cancelled out. Suppose that the amplitude x_m was in error and high. Then δ_{xm-1} would appear too high but δ_{xm} would have to be "correspondingly" too low. For this method there is an error due to experimental uncertainty and because of the use of an asymptotic solution to interpret finite measurements.

For the laminar region, "n" has the value one, which was well established experimentally when determining the laminar damping coefficients for each system (See previous section). In the turbulent regime, n is assumed to be constant

for the whole possible range of damping and its value to lie between one and two. Hence, the height of transition corresponds to the intersection of lines of slope 1 and of slope between 1 and 2 on the graph.

In each case the transition height was calculated approximately by slide rule; the data points were divided on this basis into two regions, and a least squares computer program was used to accurately determine the transition height and the turbulent damping exponent (n). Richardson's method is both easier to program and easier to use than Ury's method which involves a visual determination of the transition height from the change in slope of the graph of amplitude vs cycle time. Richardson's method involves the assumption that n is constant for the whole range of turbulent damping, or at least in the region of the transition point. Biery found that the numerically calculated velocity profiles for the first few cycles differed from those occurring subsequently. Thus, the assumption of constant n for both laminar and turbulent flow, used to mathematically describe the damping, has no real fundamental basis; but, however, seems to be an adequate approximation.

4.2.3 Theory

4.2.3.1 Boundary layer regime

Three different methods of analysis were made in order to obtain theoretical equations for the laminar-turbulent

transition in the so-called Boundary Layer Regime (i.e., $R^2\omega/\nu \geq 70$).

Derivations (i) and (ii) are an attempt to find the functional relationship between transition height and oscillation Reynolds number which Ury found to exist. Derivation (iii) is an attempt to explain the marked dependence of transition height on column length for the long one inch diameter tube (No. 4).

(i) Analogy with steady flow over a flat plate

For oscillatory flow over a flat plate the boundary layer thickness can be shown (19) to be of the order of:

$$\delta = (\nu/\omega)^{\frac{1}{2}} \tag{4.15}$$

For steady flow over a flat plate the transition Reynolds number is given by (18):

$$Re_x = \frac{ux}{\nu} \approx 500{,}000 \tag{4.16}$$

For steady flow, the boundary layer thickness (18) is:

$$\delta = 4.65\sqrt{\frac{\nu x}{u}} \tag{4.17}$$

Hence, from (4.16), the distance along the plate at which transition occurs is:

$$x = 500{,}000\ \nu/u \tag{4.18}$$

From (4.17) at transition:

$$\delta = 3300\ \nu/u \tag{4.19}$$

In the manometer system, the maximum velocity (comparable with the free stream velocity in the flat plate case) is:

$$u = \omega A \tag{4.20}$$

$$= \omega h_T \qquad \text{at transition.}$$

From (4.15) and (4.19):

$$(\nu/\omega)^{\frac{1}{2}} \approx 3300\ \nu/(\omega h_T)$$

and

$$\frac{\omega Dh_T}{\nu} = 6000 \left(\frac{R^2\omega}{\nu}\right)^{\frac{1}{2}} \tag{4.21}$$

However, if, for the transition process, the boundary layer thickness applicable is similar to that formed when the liquid accelerates from rest over a flat plate (19) then the maximum thickness (at the bottom of the stroke) would be given by:

$$\delta = 4\sqrt{\nu \frac{\pi}{\omega}} \tag{4.22}$$

$$\approx 7\sqrt{\nu/\omega}$$

and hence

$$\frac{\omega Dh_T}{\nu} \approx 930 \left(\frac{R^2\omega}{\nu}\right)^{\frac{1}{2}} \tag{4.23}$$

In both equations, (4.21) and (4.23), the essential assumption is that the laminar-turbulent transition in an oscillatory boundary layer, occurs at the same value of Re_δ as in steady flow.

(ii) Equating laminar and turbulent shear stresses

In the case of laminar boundary layer type oscillatory flow over a flat plate, the velocity distribution parallel to the wall is given by (21):

$$u(z,t) = u_o \exp\left(-z\sqrt{\frac{\omega}{2\nu}}\right)\cos\left(\omega t - z\sqrt{\frac{\omega}{2\nu}}\right) \qquad (4.24)$$

Then $$\left.\frac{\partial u}{\partial z}\right|_{z=0} = -u_o\sqrt{\frac{\omega}{2\nu}}\left(\cos\omega t + \sin\omega t\right) \qquad (4.25)$$

Therefore, the maximum laminar shear stress, at the wall occurs when $\omega t = \frac{\pi}{4}, \ldots$

and $$\tau_{lm} = -\mu\left.\frac{\partial u}{\partial z}\right|_{z=0} \qquad (4.26)$$

$$= \mu u_o \sqrt{\omega/2\nu}\,(\sqrt{2}) \qquad (4.27)$$

$$= \mu u_o \left(\frac{\omega}{\nu}\right)^{\frac{1}{2}} \qquad (4.28)$$

For fully turbulent flow through a smooth pipe, the maximum shear stress is given by the Blasius equation (18):

$$\tau_t \approx 0.0396\,\rho u^2 \left(\frac{\nu}{2uR}\right)^{-\frac{1}{4}} \qquad (4.29)$$

As for (i), the velocity for the U-tube system is $(A\omega)$.

The system will tend to occupy that flow regime in which the frictional dissipation is greater; i.e., if $\tau_t > \tau_{lm}$, then the turbulent regime will be preferred. Thus, transition occurs approximately when:

$$\tau_{lm} = \tau_t \tag{4.30}$$

It follows that:

$$\mu(h_T\omega)\sqrt{\omega/\nu} = 0.0396\rho\left(\frac{\nu}{2\omega h_T R}\right)^{\frac{1}{4}}(h_T\omega)^2 \tag{4.31}$$

$$\therefore \quad \frac{Dh_T\omega}{\nu} = 188\left(\frac{R^2\omega}{\nu}\right)^{2/3} \tag{4.32}$$

(iii) <u>As a result of wavy flow in the falling film</u>

Tallmadge and Soroka (20) experimentally determined the film Reynolds number at which the flow in a liquid film formed by the withdrawal of a plate from a trough containing the liquid became wavy:

$$Re_f = \frac{\delta_f u_R}{\nu} \approx 1 \tag{4.33}$$

In this case, the film thickness is $\sqrt{2\nu u/g}$ and so

$$\sqrt{\frac{2\nu u}{g}}\left(\frac{u}{\nu}\right) \approx 1$$

With u taken as the maximum velocity in the column during the half-cycle when transition occurs (ωh_T):

$$\sqrt{\frac{2\nu(h_T\omega)}{g}}\left(\frac{(h_T\omega)}{\nu}\right) \approx 1$$

Thus, the transition height dependence on angular frequency is:

$$h_T \propto \frac{1}{\omega} \qquad (4.34)$$

4.2.3.2 Fully developed regime

The transition from fully-developed laminar flow ($R^2\omega/\nu < 20$) to turbulence can be based directly on the same criteria for steady pipe flow (quasi-steady-state model). Thus, for the U-tube case, the maximum Reynolds number at transition is given by

$$\frac{Dh_T\omega}{\nu} \approx 2000 \qquad (4.35)$$

4.2.4 Discussion

4.2.4.1 Method of analysis

The analysis of manometer responses, using Richardson's (12) method, for three typical runs is shown in Figs. 4, 5 and 6. In the first case, a mercury/glass system, there is no liquid film formed on the tube, and consequently, the equilibrium

position of the column remains constant throughout the oscillations. The experimental results seem to be fitted by Richardson's method better in the turbulent regime than for laminar flow. The initial starting height does not significantly affect the results. The apparent large scatter in the laminar region is due to taking the logarithm of the ratio of two similar numbers, in which case a small experimental error in one reading is greatly magnified in the corresponding logarithmic ratio. Consider three typical heights occurring for an initial height of six inches; namely, 1.57, 1.34, and 1.11 inches. This raw data gives logarithmic decrements of 0.070 and 0.083, hardly constant as would be expected in the laminar regime. Now the experimental error is estimated at 0.02 inches, thus, the middle height may have actually been 1.32 inches rather than the 1.34 inches recorded. In this case, the decrements would have been 0.076 and 0.075, which are close to the average for all laminar readings of 0.077. Hence, by taking the average of a large number of readings an accurate average logarithmic decrement for use in determining the transition height was found. However, because the amplitudes are larger for turbulent damping, the same experimental error (0.02 inches) produces a considerably smaller inaccuracy in the corresponding amplitude ratio, leading to apparently more accurate results in the turbulent region.

In Fig. 5 the system was water/glass where a very irregular and non-uniform liquid film was formed at high amplitudes. This is shown in the results by the large experimental scatter in the turbulent region when comparing runs with different starting heights. The results in the laminar region (a more uniform film, but still irregular compared with other solutions) are more reliable. In general, the results for water are possibly the most inaccurate due to the effect of the irregular liquid film on damping. Thus, in the case of water, in particular, the internal geometry and nature of the tube surface would have a significant effect on the degree of damping and the transition height.

For the toluene-paraffin/glass system, Fig. 6, the results are similar to those for water/glass. However, in the turbulent regime, the results for each individual run (the same starting height) show less scatter and indicate that the initial height, because of its subsequent effect on film thickness and length, does influence the damping in the turbulent regime.

In general, Richardson's method of analysis worked well for all of the 25 runs. Experimental evidence seems to substantiate the assumption that the turbulent damping exponent (n) is constant, at least over the range of amplitudes investigated, which in practice, is limited by the column length.

FIGURE 4: TRANSITION HEIGHT DETERMINATION

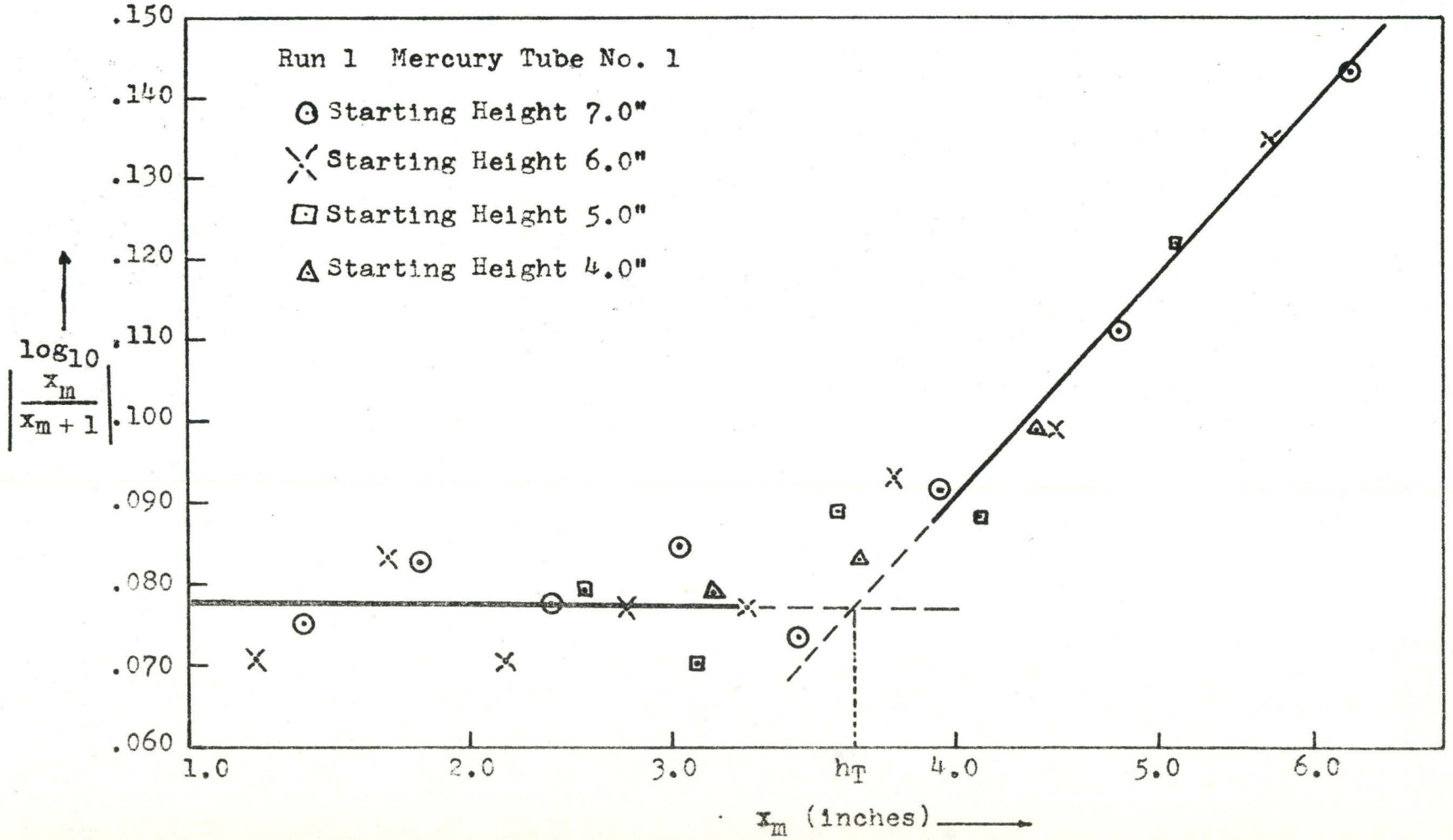

FIGURE 5: TRANSITION HEIGHT DETERMINATION

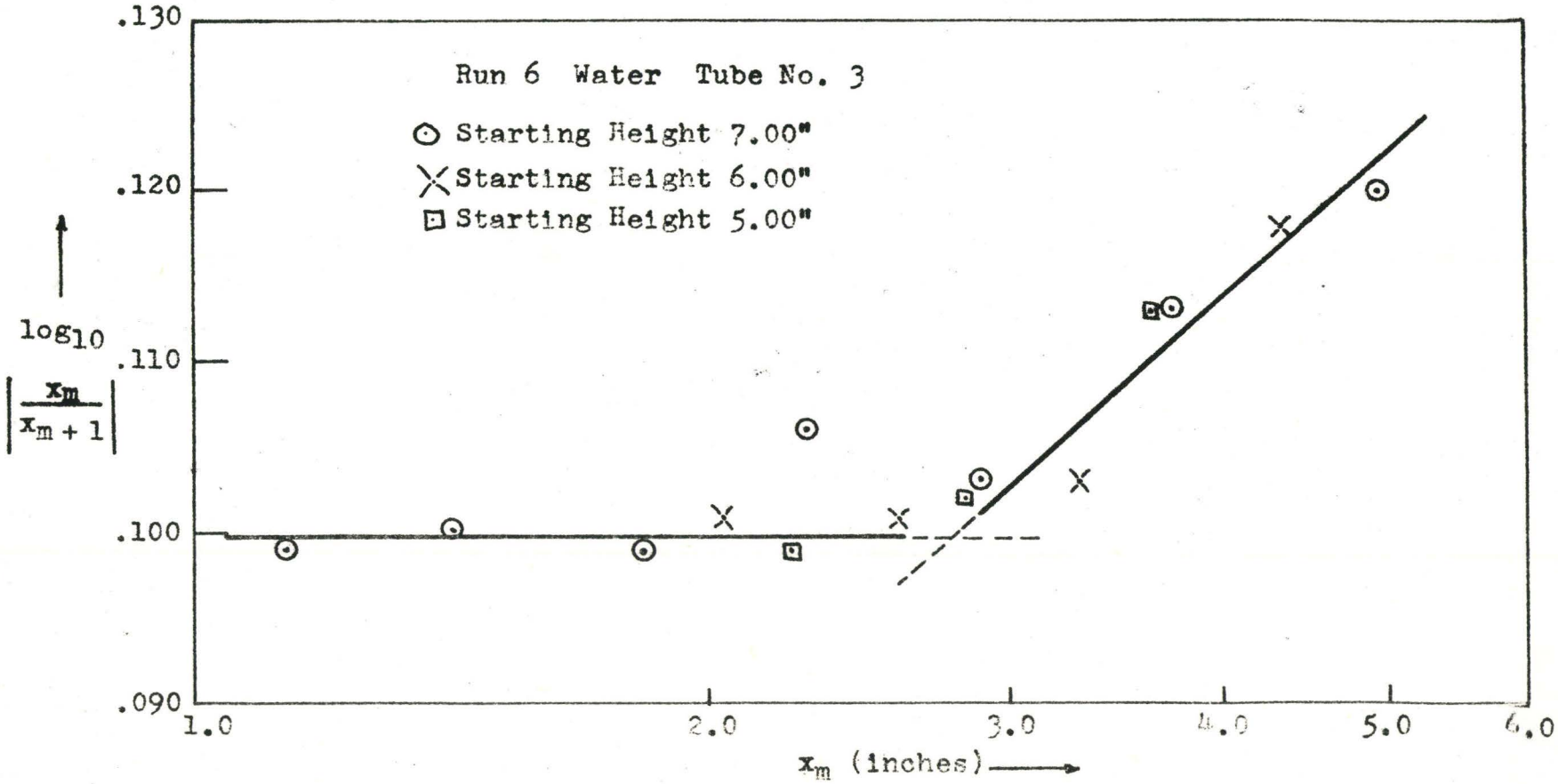

FIGURE 6: TRANSITION HEIGHT DETERMINATION

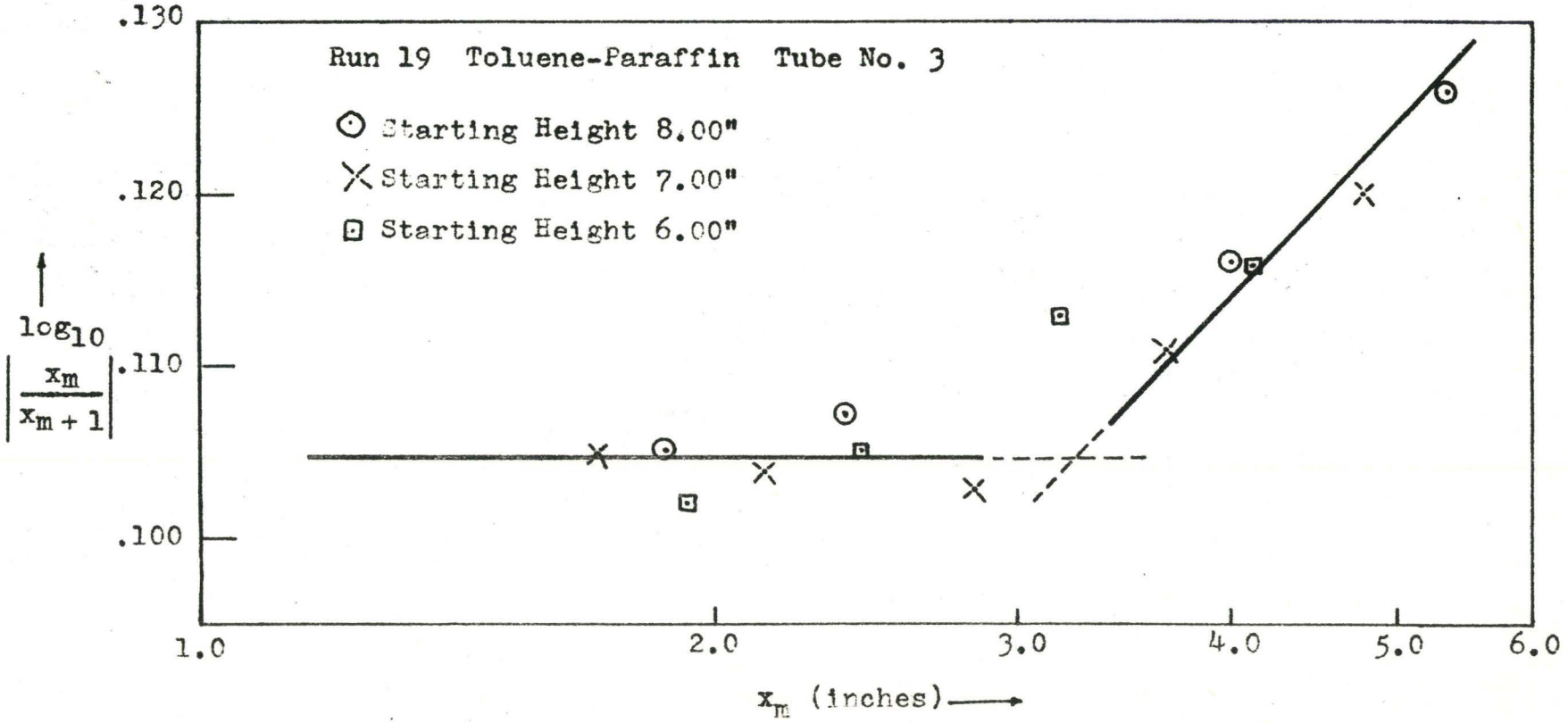

4.2.4.2 Transition Reynolds number

A graphical method of presenting the transition results using dimensionless parameters (Reynolds numbers), similar to that used by Baird (14) in correlating the onset of separation during pulsed flow past a cylinder, was used. As in the presentation of damping factor data for laminar flow, $R^2\omega/\nu$ was chosen as the basic parameter for a comparison of various systems.

As the transition from laminar to turbulent flow has been studied less extensively than the transition from fully-developed to boundary layer flow in oscillatory laminar flow, the choice of a parameter to represent this transition was more difficult. Initially, with a large initial displacement in the U-tube, the flow is of a turbulent nature. As the amplitude of the oscillations decreases, due to fluid damping, there is a height (h_T) at which transition to a laminar damping characteristic occurs. The Reynolds number chosen to represent this transition was the maximum occurring during the cycle, namely:

$$Re_T = \frac{D h_T \omega}{\nu} \qquad (4.36)$$

This Reynolds number is similar to the one used to describe the same transition in steady pipe flow. In the unsteady U-tube cases, the velocity used, ($h_T \omega$), is the maximum one during the oscillation cycle in which transition occurs.

A linear regression of the results for the 25 experimental runs is shown in Fig. 7, together with the semi-theoretical equations derived previously. It can be seen that the line of best fit for all the results is in good agreement with equation (4.32) which is based on equating turbulent and laminar wall shear stresses at the transition point. In particular, the experimental slope of 0.66 compares well with the theoretical value of 2/3. However, because of the large apparent experimental scatter, this encouraging overall result may be solely due to the favourable compensating of experimental errors. The division of the results into smaller groups for a more detailed analysis will be discussed later.

There is very little published data with which to compare these results. Also, as the geometric features of the particular systems greatly influence the turbulent/laminar transition point, a valid comparison would be difficult to make. For oscillation Reynolds numbers in the range 200-1000 the transition Reynolds number ($Dh_T \omega/\nu$), determined from these experiments, is of the same order of magnitude (10^4) as for the results of Ury, Richardson and Biery. Run 8 for water compares most favourably with that obtained in a smaller diameter tube by Biery ($R^2 \omega/\nu = 570$). However, he makes no mention of the method of determining transition height used, though it appears as if it was Richardson's method of analysis.

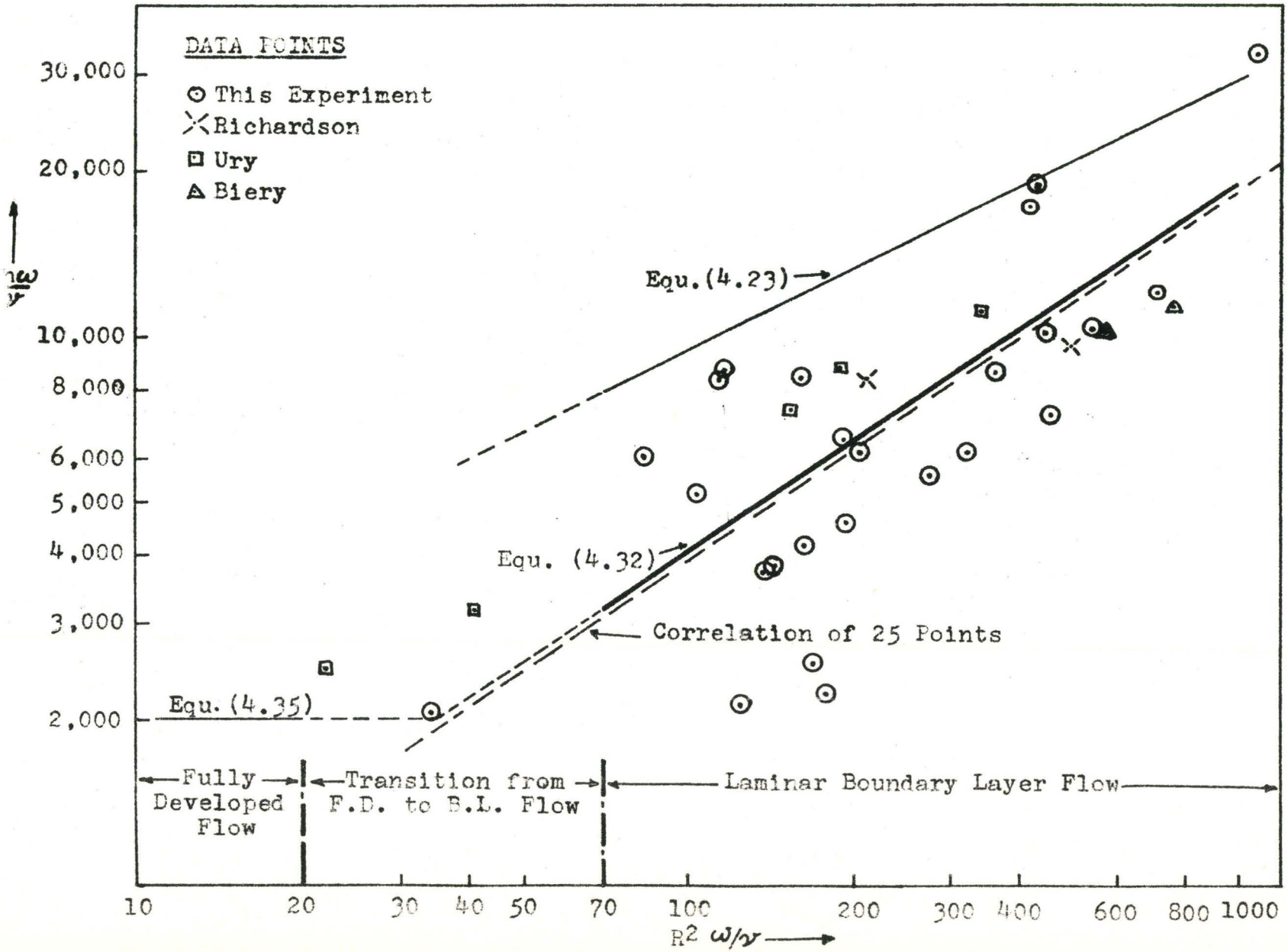

FIGURE 7: TRANSITION REYNOLDS NUMBER vs. OSCILLATION REYNOLDS NUMBER

One general trend is that mercury appears to give larger than average transition heights, possibly due to abnormal surface tension effects at the column ends. The results for Runs 1, 2 and 3, are similar to Ury's mercury results. Ury's method of determining the transition height was to visually detect the change in slope, resulting from transition from turbulent to laminar flow, for a plot of amplitude height vs cycle time. This method certainly is more difficult to use as the plot is a curve and the change in slope is not sharp, but actually occurs over a range of heights. With Richardson's method, the intersection of the two straight lines yields just one transition point, but, as previously mentioned, this method inherently assumes that the turbulent damping exponent is constant over the whole range of turbulent oscillations. Due to experimental errors involved, because of the end effects previously mentioned in the discussion of laminar damping, Ury's analysis seems to yield equally meaningful results, in particular, the similarity for mercury.

Increasing the column length, holding other factors constant, has a marked effect on the transition height as indicated by the water and toluene results in the long one inch diameter tube (Fig. 11). The onset of wavy flow in the falling film, and the influence of the turbulent damping exponent in general, as a possible explanation of this observation will be discussed later.

As the turbulent damping exponents for Runs 14, 21, 22, 23 and 24 are very low, the transition height given by the analysis may not be an actual turbulent-laminar transition, but rather due to a change in the laminar damping coefficient with successive oscillations. It is noticed that all these runs are with large diameter tubes (1.50" and 1.90") and hence, the velocity profile in laminar flow near the free surfaces would take a while to establish itself, as verified by Biery's numerically calculated profiles. This may be the reason for the apparently very low transition Reynolds numbers for Runs 23 and 24.

Run 25 at low oscillatory Reynolds number ($R^2 \omega/\nu = 32$) together with Ury's results for water indicates that a minimum transition Reynolds number of 2000 is approached as $R^2 \omega/\nu$ is decreased and the Quasi-Steady-State model begins to apply.

In the turbulent regime it was found that the damping for the first half-cycle was greatly increased above the expected value (from extrapolation of results). Consequently, the first point was not used in the analysis of transition height. The one exception was Run 16 with methanol. In this case only the first half-cycle of the oscillations was used and the starting height varied. This run yielded both a higher turbulent damping exponent and a correspondingly larger transition height. This was the first sign of the relation between turbulent damping on transition.

4.2.4.3 Classification of data

Fig. 7 seems to imply a very large experimental scatter for transition heights. The experimental error in the transition Reynolds number was estimated at about ± 20%. However, further analysis of the results showed that the turbulent damping exponent (n of equation 4.10) varied greatly between the 25 runs. For fully developed turbulent flow, an exponent in the range 1.70 - 2.0 would be expected. However, it was found that this occurred only in two cases, indicating that the assumption of a sharp transition to fully developed turbulence may not be valid for a number of the U-tube systems. To aid in the further analysis of the results, the experimental runs were divided into three groups thus:

(i) $n \geqslant 1.35$

(ii) $1.20 < n < 1.35$

(iii) $n \leqslant 1.20$

and each group of results correlated using a least squares analysis. The results are presented in Fig. 8 and Table 2.

As seen from Fig. 8, the scatter in the experimental results has been substantially reduced by classifying the data, with respect to the relevant turbulent damping exponent range, prior to analysis. Now all the results (except for the two runs, 23 and 24, with low exponents) deviate from the correlation equations by an amount well within the magnitude of the experimental error (± 20%). The slopes for two of

FIGURE 8: TRANSITION REYNOLDS NUMBER

vs. OSCILLATION REYNOLDS NUMBER FOR CLASSIFIED DATA

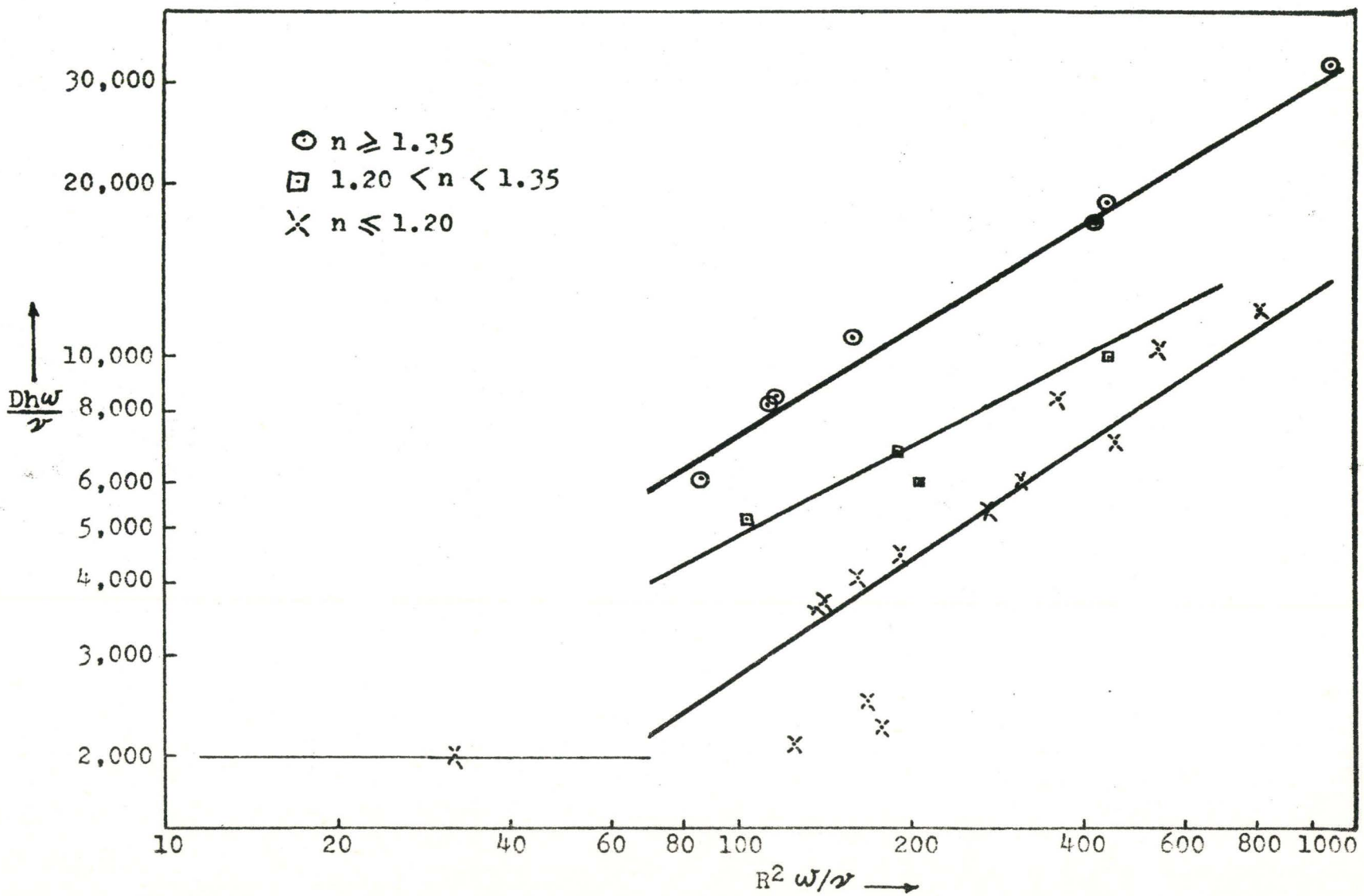

the groups (0.67 and 0.62) agree favourably with the semi-theoretical value of 2/3 and it must be remembered that there were only four points in group 2 and also in this case a slope of 2/3 would fit the data within experimental error. Hence, the importance of the turbulent damping exponent for flow prior to transition to laminar flow has been well established. This may suggest that both fully-developed and boundary flow regimes, which have been well established for laminar flow, exist in turbulent damping in U-tubes.

TABLE 2

VALUE OF n	NO. OF POINTS	VALUE OF $Dh_T \omega/\nu$ AT $R^2 \omega/\nu = 100$	SLOPE OF LINE
1.0 - 2.0	25	3,800	.66
1.35 - 2.0	7	7,060	.62
1.20 - 1.35	4	4,810	.47
1.0 - 1.20	14	2,740	.67

4.2.4.4 Turbulent damping exponent

A first attempt to explain the low turbulent damping exponents occurring in a majority of the cases, was based on the analysis of the build-up of a velocity profile in the entrance section during steady flow through a pipe. It was hoped that this may be analogous to the production of a velocity profile when the meniscus of the column begins to move in oscillatory flow in the manometer, i.e., a quasi-steady-state comparison.

For laminar flow in the pipe entrance section, the initially flat profile gradually transforms to a fully developed parabolic profile as the boundary layer grows. The distance downstream at which the profile is fully developed is given by (19):

$$x = 0.04 \left(\frac{R^2 u}{\nu} \right)$$

For a Reynolds number of 2000 then, and a tube diameter of 1 cm, a column length of 80 cm would be required to fully develop a velocity profile. Hence, from this approximate analysis, it would appear that the velocity profile may not be fully developed, even for turbulent damping where the column length is small.

The qualitative nature of this conclusion is substantiated by Fig. 9 and 10. In Fig. 9, for a constant column length, the turbulent damping exponent increases as the diameter is decreased. Assuming that the turbulent boundary

FIGURE 9: TURBULENT DAMPING EXPONENT
vs. TUBE DIAMETER

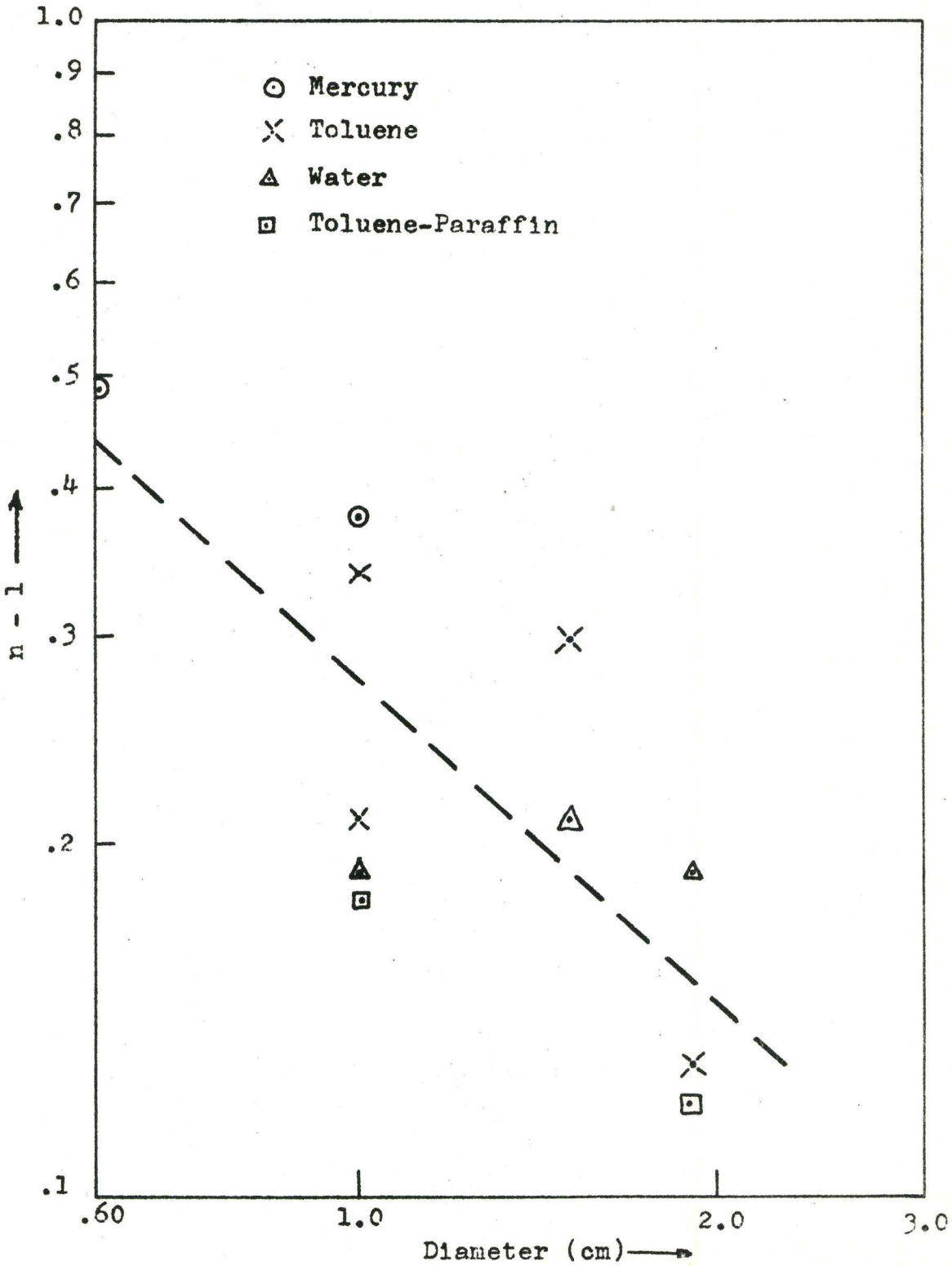

FIGURE 10: TURBULENT DAMPING EXPONENT
vs. OSCILLATION PERIOD

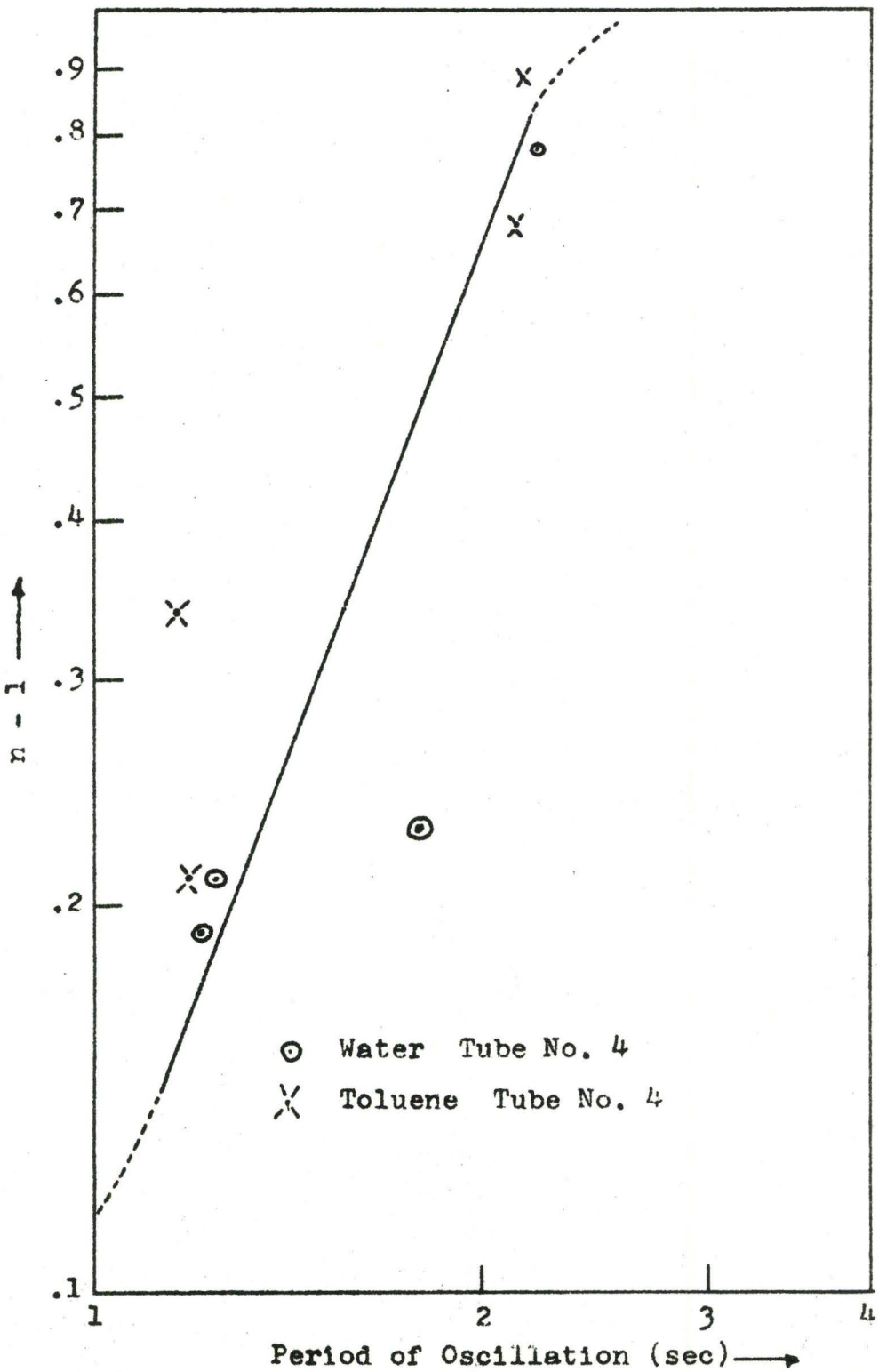

layer is of a similar size for each case, then a fully developed profile is more closely achieved in small diameter tubes. In Fig. 10, for a constant tube diameter, the exponent increases as the period of oscillation increases (due to increasing the column length). As expected, the longer columns and longer oscillation period, give more opportunity to develop the velocity profile and hence, the damping exponent is larger. Thus, to summarize, the results indicate that wherever more opportunity is given to develop the velocity profile fully (small diameter, long column) the value of n in the turbulent damping equation is higher.

However, when different fluids were compared, with respect to the size of the boundary layer (a function of viscosity) to be expected, the analysis broke down. This indicates that the effect of surface tension on end effects may also be important in determining the damping exponent, and viscosity to be less important in the turbulent regime.

4.2.4.5 Wavy flow

Fig. 11, shows that for larger liquid columns, the column length (shown through its relationship with frequency) has a far more substantial effect on transition height than would be expected.

From equation (4.32) the proportionality between transition height and frequency (for same tube diameter and solution) is:

FIGURE 11: TRANSITION HEIGHT vs. FREQUENCY
(TUBE NO. 4)

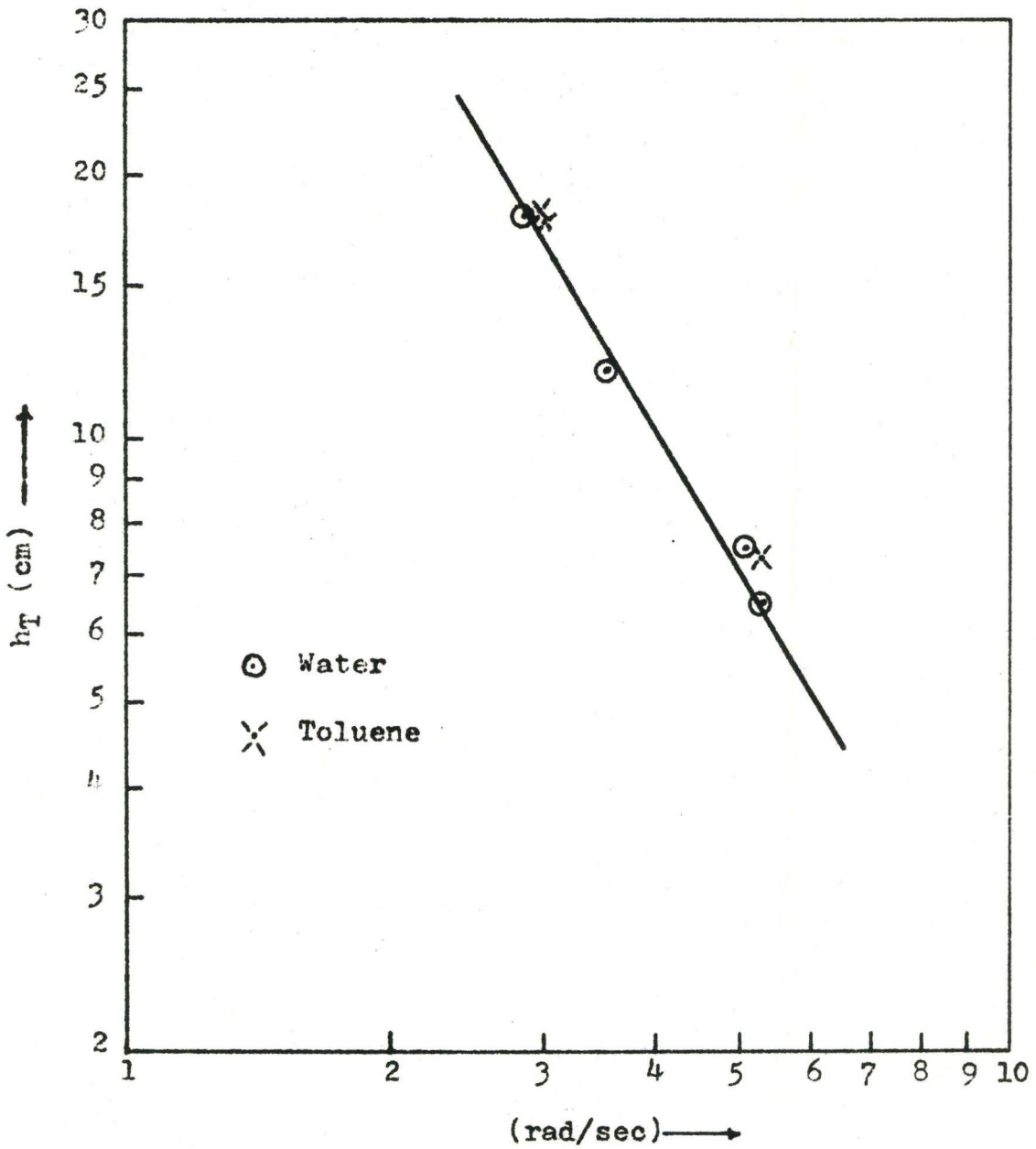

$$h_T \propto \omega^{-1/3}$$

If transition is due to wavy flow in the liquid film adhering to the tube wall, for long columns, then from equation (4.34)

$$h_T \propto \omega^{-1}$$

In practice, it was found that (From Fig. 11):

$$h_T \propto \omega^{-1.7}$$

As previously indicated, this marked dependence on column length is accompanied by a change in the value of n for turbulent damping. This in itself is the most conclusive evidence that transition is dependent on two factors, i.e., the oscillatory Reynolds number for the system, and the value of the damping exponent for the turbulent flow prior to transition. The results give inconclusive evidence as to the effect of the type of flow in the adhering fluid film, on the transition phenomena.

5. CONCLUSIONS AND RECOMMENDATIONS

(i) Secondary end effects are probably responsible for increasing the laminar damping coefficient by up to 15% above the theoretical asymptotic solutions, which are based solely on the primary fluid flow patterns. Biery's (7) numerical solution gives the best fit of the results, and the laminar damping factors for all 25 runs agree extremely well with those obtained experimentally by previous workers.

(ii) Transition in oscillatory flow can be adequately summarized in the form of a log - log plot of transition Reynolds number ($Dh_T \omega/\nu$) vs. oscillation Reynolds number ($R^2\omega/\nu$). For laminar flow the transition from a fully developed profile to one of boundary layer nature has been well-established for the range (10)

$$20 \leq Re_o \leq 70$$

The transition from laminar to turbulent flow for $Re_o > 70$ is not as well defined and seems to depend on the turbulent damping exponent for the flow prior to transition. Also, the transition seems to be influenced by the internal tube geometry and by end effects. The relationship between turbulent damping

exponent and transition suggests the possibility of both fully developed and boundary layer regimes of turbulent flow, as with laminar flow.

For $Re_o < 70$, the limited data available suggests that the transition Reynolds number approaches the steady-state value of 2000.

(iii) It is recommended that further experimental runs with large diameter tubes of different radii of curvature be made, to investigate the importance of viscous dissipation in the curved section, on laminar damping. Also, further experiments at low oscillation Reynolds numbers ($Re_o < 70$), to check the validity of the Quasi-Steady-State model are needed.

NOMENCLATURE

General Symbols

A	amplitude of oscillations
b	coefficient in laminar damping equation (4.1)
D	tube diameter
F	forcing function in laminar damping equation (4.1)
f	friction factor
g	gravitational constant
h	characteristic U-tube displacement
h_f	apparent increase in column displacement
j	coefficient in laminar damping equation (4.1)
L	length of liquid column
n	damping exponent for turbulent flow
r	radial position
R	tube radius
Re	Reynolds numbers $Dh\,\omega/\nu$
Re_f	for film $\delta_f u_R/\nu$
Re_k	Ury's modified kinetic Reynolds number
Re_h	Richardson's kinematic Reynolds number $h^2\,\omega/\nu$
Re_o	oscillation Reynolds number (Valensi's number) $R^2\,\omega/\nu$
Re_p	pipe Reynolds number Du_m/ν

General Symbols

Re_T	transition Reynolds number (U-tube) $Dh_T \omega/\nu$
Re_x	transition Reynolds number (flat plate) ux/ν
t	time
u	liquid velocity parallel to plate
u_m	mean velocity, taken over cross-section of tube
u_o	maximum liquid velocity in x direction
u_R	relative fluid velocity for plate withdrawal
x	characteristic dimension along surface
x_m	oscillation peak height
z	direction perpendiculat to surface

Subscripts

c	curvature
d	driving force
f	film
i	initial
lm	laminar
t	turbulent
T	transition

Greek Symbols

Γ	gamma function
δ	boundary layer thickness
δ'	Ury's mass factor

Greek Symbols

δ_f	film thickness
δ_{xm}	logarithmic decrement
Δ	logarithmic decrement
ζ	laminar damping coefficient
μ	dynamic liquid viscosity
ν	kinematic liquid viscosity
ρ	liquid density
τ	shear stress
ω	angular frequency
ω_n	natural angular frequency $(2g/L)^{\frac{1}{2}}$ of oscillation.

BIBLIOGRAPHY

1. M.M. MENNERET. J. Phys. théor. Appl. 1, 753 (1911).
2. J. VALENSI. C.R. Acad. Sci. Paris, 224, 446 (1947).
3. J. VALENSI and C. CLARION. Ibid. 224, 532 (1947).
4. E.G. RICHARDSON and E. TYLER. Proc. Phys. Soc. London 42, 1 (1929).
5. T. VON KARMAN and J. VALENSI. C.R. Acad. Sci. Paris, 227, 105 (1948).
6. J.F. URY. Int. J. Mech. Sci. 4, 349 (1962).
7. J. BIERY. A.I. Ch. E.J. 9, 606 (1963).
8. J. BIERY. Ibid. 10, 551 (1964).
9. P.D. RICHARDSON. Int. J. Mech. Sci. 5, 415 (1963).
10. P.D. RICHARDSON. A.I. Ch.E.J. 13, 823 (1967).
11. E.R. LINDGREN. Arkivfysik. 12, 1 (1957).
12. P.D. RICHARDSON. J. Roy. Aeron. Soc. 68, 846 (1964).
13. A.M. BINNIE. Proc. Phys. Soc. London, 57, 390 (1945).
14. M.H.I. BAIRD. Chem. Eng. Sci. 22, 1056 (1967).
15. J. VALENSI and C. CLARION. C.R. Acad. Sci. Paris, 226, 554 (1948).
16. J. VALENSI et al. Ibid. 230, 2002 (1950).
17. J.H. PERRY. Chemical Engineers Handbook: McGraw-Hill
18. R.B. BIRD et al. Transport Phenomena: J. Wiley (1960).

19. H. SCHLICHTING. Boundary Layer Theory: McGraw-Hill (1962).

20. J.A. TALLMADGE and A.J. SOROKA. Chem Eng. Sci. 24, 377 (1969).

21. G.K. BATCHELOR. An Introduction to Fluid Dynamics: Cambridge University Press (1967).

22. D.G. CHRISTOPHERSON. et al. Proc.Roy.Soc. A168, 351 (1938).

APPENDICES

APPENDIX I

A.1 VISCOSITY MEASUREMENT

A capillary viscometer was used to determine the kinematic viscosity of the toluene-paraffin mixtures. This apparatus consisted of a vertically mounted 50 ml burette which was connected to a 40 cm length of 1 mm diameter capillary tubing fixed horizontally. For this system the flow rate of liquid in the capillary, for Newtonian fluids is given by (18):

$$Q = \frac{\pi R^4 \Delta p}{8 \mu l} = - A \frac{dh}{dt} \qquad (i)$$

where R = capillary radius

Δp = pressure drop across capillary

l = capillary length

A = cross-section area in burette

h = liquid height above capillary

Now $$\Delta p = \rho g h \qquad (ii)$$

Thus $$\frac{\pi R^4 \rho g h}{8 \mu l} = - A \frac{dh}{dt} \qquad (iii)$$

As the geometric factors are kept constant for all measurements:

$$\frac{dh}{dt} = - K \frac{h}{\nu} \qquad \text{(iv)}$$

Hence $$\ln h = - \frac{K}{\nu} t + c$$

where K,c are constants for the system, which are determined by calibrating with water.

The viscosity of the toluene-paraffin mixture was obtained then from the slope of ln h vs time graphs, the linear nature of the plot verifying that the mixtures were Newtonian.

APPENDIX II

TABLE 1: DATA

RUN	FLUID	TEMP °C	PERIOD sec	TUBE No	VISCOSITY cm^2/sec	h_T cm	$R^2\omega/\nu$	$Dh\omega/\nu$	n
1	Mercury	16.0	1.10	1	.00118	6.35	436	18,500	1.50
2	Mercury	24.5	1.15	2	.00117	6.10	421	17,100	1.56
3	Mercury	20.0	1.17	3	.00117	7.03	1150	32,200	1.38
4	Water	26.8	2.20	4	.00860	18.03	83	5,940	1.78
5	Water	27.8	1.79	4	.00840	12.48	104	5,210	1.23
6	Water	24.2	1.21	3	.00910	6.57	143	3,750	1.19
7	Water	18.5	1.24	5	.0104	7.51	273	5,460	1.20
8	Water	26.2	1.21	6	.00870	9.21	573	10,400	1.19
9	Toluene	27.0	2.12	4	.00645	17.94	115	8,230	1.68
10	Toluene	28.7	2.14	4	.00635	18.23	116	8,440	1.89
11	Toluene	22.0	1.15	3	.00682	8.42	192	6,460	1.34
12	Toluene	24.7	1.18	3	.00647	7.36	206	6,050	1.20
13	Toluene	22.5	1.19	5	.00670	8.58	443	10,100	1.30
14	Toluene	24.0	1.21	6	.00664	8.19	704	12,100	1.13
15	Methanol	26.3	1.18	3	.00695	5.89	191	4,510	1.19
16	Methanol*	19.0	1.15	3	.00858	13.07	159	8,320	1.42
17	Tol-Par**	26.4	1.19	3	.00821	6.39	161	4,100	1.17
18	Tol-Par	26.4	1.19	5	.00821	8.81	362	8,500	1.17
19	Tol-Par	26.8	1.17	3	.00975	6.63	138	3,660	1.18
20	Tol-Par	27.5	1.19	5	.00958	7.39	310	6,110	1.20
21	Tol-Par	24.0	1.20	6	.0104	7.48	455	7,170	1.12
22	Tol-Par	26.3	1.20	5	.0235	6.30	125	2,110	1.18
23	Tol-Par	24.6	1.25	6	.0270	7.25	168	2,560	1.13
24	Tol-Par	24.7	1.20	6	.0270	6.05	178	2,270	1.14
25	Tol-Par	28.7	2.19	4	.0225	15.71	32	2,000	1.18

* Only first half-cycle used

** Toluene-Paraffin

TABLE 2: OSCILLATION HEIGHTS

RUN NO.	1	2	3	4	5	6
	7.00*	6.04*	7.00*	7.82*	5.95*	7.00*
	5.27	4.22	6.07	5.75	4.48	4.91
	3.80	3.27	4.88	4.27	3.45	3.73
	2.95	2.64	4.08	3.17	2.63	2.88
	2.40	2.22	3.45	2.35	2.02	2.27
	2.03	1.92	3.06			1.78
	1.68	1.67		9.65*	6.84*	1.42
	1.41	1.46	6.00*	6.52	5.10	1.13
	1.17	1.25	5.32	4.85		0.90
	0.99		4.33			
		5.42*	3.67	11.65*		6.00*
	5.00*	3.92	3.15	7.45		4.31
	4.12	3.07	2.83			3.29
	3.12			10.25*		2.58
	2.55		4.00*	6.75		2.04
	2.08		3.67	5.04		1.62
	1.77		3.17			
	1.48		2.84			5.00*
			2.51			3.63
	6.00*		2.27			2.82
	4.72		2.02			2.23
	3.48		1.80			1.78
	2.76		1.67			
	2.23		1.53			
	1.87					
	1.57		3.00*			
	1.34		2.77			
	1.11		2.47			
	0.94		2.23			
			2.02			
	4.00*		1.78			
	3.37		1.64			
	2.63		1.49			
	2.18		1.34			
	1.82		1.23			
			1.11			
			.99			

*signifies starting height for subsequent oscillations

TABLE 2 (Cont.)

RUN NO.	7	8	9	10	11	12
	6.00*	8.00*	13.00*	10.45*	7.00*	7.00*
	4.65	6.68	8.50	7.05	5.15	5.17
	3.82	5.57	6.30	5.48	3.98	4.06
	3.17	4.83	4.87	4.28	3.10	3.25
	2.68	4.23	3.75	3.35	2.58	2.66
	2.30	3.73		2.63	2.10	2.17
	1.93	3.32	11.85*	2.09	1.68	1.78
	1.65	2.94	7.95	1.63	1.40	1.46
	1.42	2.62	6.00		1.12	
	1.20	2.34		12.72*		8.00*
	1.02	2.08	10.30*	8.20		5.82
			7.37	6.25		4.43
		7.00*	5.57			3.52
		5.88	4.32	11.60*		2.85
		5.04		7.70		2.34
		5.36		5.95		1.92
		3.82				1.58
		6.00*				
		5.12				
		4.41				
		3.87				
		3.42				

TABLE 2 (Cont.)

RUN NO.	13	14	15	16	17	18
	6.00*	7.00*	7.00*	-8.00*	7.00*	6.00*
	-5.38	6.04	5.17	5.65	5.05	4.80
	4.18	5.22	4.03	-7.00	3.85	4.06
	-3.90	4.59	3.18	4.95	3.02	3.45
	3.15	4.09	2.56	-6.00*	2.39	2.97
	-2.97	3.64	2.10	4.37	1.97	2.55
	2.42	3.26	1.72	-5.00	1.55	2.18
	-2.30	2.95	1.42	3.82	1.23	1.88
	1.85	2.66	1.18	-4.00*		
		2.40	0.97	3.06	6.00*	7.00*
	-6.00*	2.17		-3.00*	4.40	5.54
	4.95	1.96	6.00*	2.30	3.42	4.62
	-4.52		4.57	-2.00*	2.66	3.87
	3.58	6.00*	3.59	1.52	2.11	3.30
	-3.35	5.19	2.86		1.66	
	2.74	4.58	2.32		1.34	
	-2.58	4.06	1.90		1.08	
	2.10	3.62	1.57			
	-2.05	3.26				
			8.00*			
		5.00*	5.81			
		4.43	4.43			
		3.94	3.51			
		3.52	2.82			

TABLE 2 (Cont.)

RUN NO.	19	20	21	22	23	24	25
	8.00*	6.00*	6.00*	7.00*	7.00*	7.00*	5.03*
	5.36	4.72	5.04	4.82	5.24	4.73	2.75
	4.00	3.92	4.33	3.56	4.12	3.48	1.52
	3.06	3.27	3.76	2.68	3.28	2.59	.84
	2.39	2.75	3.28	2.07	2.64	1.97	.46
	1.87	2.35	2.88	1.60	2.13	1.51	
	1.47	2.03	2.54	1.24	1.74	1.15	7.10*
		1.73	2.24	0.96	1.42		3.85
	6.00*	1.48	1.98		1.15	6.00*	2.10
	4.13		1.75	6.00*		4.13	
	3.17	8.00*	1.54	4.17	6.00*	3.06	9.30*
	2.45	6.32		3.13	4.52	2.32	4.93
	1.93	5.05	5.78*	2.37	3.58	1.77	
	1.53	4.14	4.93		2.87		8.55*
		3.48	4.25		2.33	5.00*	4.60
	7.00*		3.70		1.88	3.53	
	4.82		3.23			2.62	7.95*
	3.66				5.00*	1.98	4.30
	2.76				3.82		
	2.18				3.06		
	1.72				2.48		
	1.35				2.02		